CHAPTER 1

An Introduction to the Basic Principles and Concepts of Mass Spectrometry

Kym F. Faull, Alek N. Dooley, Frederic Halgand, Lorelei D. Shoemaker, Andrew J. Norris, Christopher M. Ryan, Arthur Laganowsky, Jodie V. Johnson and **Jonathan E. Katz**

Contents

1.	Opening Remarks	2
2.	The Instrument	4
3.	Vacuum Systems	4
4.	Definitions	5
5.	Resolution	6
6.	Mass Accuracy	8
7.	Isotopes	9
8.	Reconciling Theoretical and Measured Masses	11
9.	Charge State Assignment	11
10.	The Need for Chromatography	12
11.	The Myth of Defining Elemental Compositions	13
12.	Desorption Ionization: Laser Desorption	14
13.	Spray Ionization: Electrospray Ionization	16
14.	Mass Analyzers	19
15.	Time-of-Flight Mass Spectrometers	20
16.	Linear Quadrupole Mass Filters	22
17.	Quadrupole Ion Traps	23
18.	Linear Ion Traps	26
19.	Ion Cyclotron Cells and Fourier Transform Mass Spectrometry	27
20.	The Orbitrap	29
21.	Detectors	30
22.	Electron Multipliers	31
23.	Conversion Dynodes or High-Energy Dynodes	32
24.	Quantification	32
25.	Structural Elucidation by Mass Spectrometry	34
26.	Gas Phase Ion Stabilities and Energetics of the Collisionally-Activated Dissociation Process	35

Comprehensive Analytical Chemistry, Volume 52
ISSN: 0166-526X, DOI 10.1016/S0166-526X(08)00201-8

27. Collision-Induced Dissociation 36
28. Electron Capture Dissociation 38
29. Electron Transfer Dissociation 40
30. Scan Modes in Tandem Mass Spectrometry 40
31. Conclusions 43
Acknowledgements 44
References 44

1. OPENING REMARKS

The definition of mass spectrometry as the science of manipulating gas phase ions identifies the physical technique with which this volume is concerned [1]. If a molecule can be converted into a gas phase ion it can be interrogated by this technique. Making possible the study of proteins by mass spectrometry required the development of methods to convert them into gas phase ions, and techniques to separate the ions and detect them. At first this seemed an impossible task. How can a delicate polymeric chain of chemically dissimilar amino acids — which may contain thousands of carbon, nitrogen, oxygen, sulfur and phosphorous atoms — that is thermally unstable and has negligible vapor pressure, be converted into a gas phase ion? The processes involved, however, are astonishingly straightforward. In this opening chapter the reader is introduced to the principles of these processes as a prelude to the more detailed and complex chapters that follow.

The technique of mass spectrometry began with the work of Thomson, Dempster and Aston [2] in the early 1900s. Since then, the field has grown in an exponential manner, spurred on by several major developments. The literature is replete with many accounts of these developments; a particularly unique perspective is provided by Brunnée [3]. Combined gas chromatography-mass spectrometry was one of these developments in the 1960s. It allows for the direct analysis of complex mixtures, thus obviating the prior need for sample purity. This development more or less coincided with the use of the technique to monitor contamination of the environment with man-made chemicals including pesticides and other pollutants. Another significant development came in the 1970–1980s when the first desorption ionization techniques were introduced. Thermal stability was not necessary for successful ionization with these ionization methods. The so-called *plasma desorption* and *fast atom bombardment* ionization techniques, stemming from the work of Macfarlane [4] and Barber [5] and their colleagues, respectively, stand out as being particularly significant developments. These developments provided an inspirational lead for others to follow, and the subsequent discoveries of laser desorption (LD) and electrospray ionization (ESI), for which Tanaka [6], Karas and Hillenkamp [7] and Fenn [8] are widely acknowledged, provided robust ionization methods for a wide range of

both thermally stable and thermally unstable molecules including proteins and peptides. The chapters in this volume bear testimony to the significance of these discoveries.

Amino acids, peptides and proteins have several unique characteristics which make them particularly suitable to mass spectrometric analysis. Firstly, their ionizable functionalities render these molecules excellent candidates for ESI and LD ionization. Secondly, with the exception of isoleucine and leucine (Table 1), the unique masses of 18 of the 20 common protein amino acids allows for identification on the basis of their mass alone. Thirdly, the universal amide bond that links the amino acids means that the characterization of polymers of amino acids is not confounded with complications that arise from linkage heterogeneity, as is the case with carbohydrate characterization. Known rare exceptions to this third point include the isoaspartyl and isodityrosine bonds that occur in some mammalian proteins and peptide cross-linkages that occur in some bacterial cell wall proteins.

Table 1 The amino acids of proteins

Amino acid[a]	Three letter symbol	Single letter symbol	Residue molecular weights (Da)		
			Integer	Average	Monoisotopic
Alanine	Ala	A	71	71.0788	71.03711
Arginine	Arg	R	156	156.1876	156.10111
Asparagine	Asn	N	114	114.1039	114.04293
Aspartic acid	Asp	D	115	115.0886	115.02694
Cysteine	Cys	C	102	103.1448	103.00919
*Glutamine	Gln	Q	128	128.1308	128.05858
Glutamic acid	Glu	E	129	129.1155	129.04259
Glycine	Gly	G	57	57.0520	57.02146
Histidine	His	H	137	137.1412	137.05891
**Isoleucine	Ile	I	113	113.1595	113.08406
**Leucine	Leu	L	113	113.1595	113.08406
*Lysine	Lys	K	128	128.1742	128.09496
Methionine	Met	M	131	131.1986	131.04049
Phenylalanine	Phe	F	147	147.1766	147.06841
Proline	Pro	P	97	97.1167	97.05276
Serine	Ser	S	87	87.0782	87.03203
Threonine	Thr	T	101	101.1051	101.04768
Tryptophan	Trp	W	186	186.2133	186.07931
Tyrosine	Try	Y	163	163.1760	163.06333
Valine	Val	V	99	99.1326	99.06841

[a]Amino acids have unique masses. The exception is isoleucine and leucine (**), which have identical elemental composition. Lysine and glutamine (*) have similar masses.

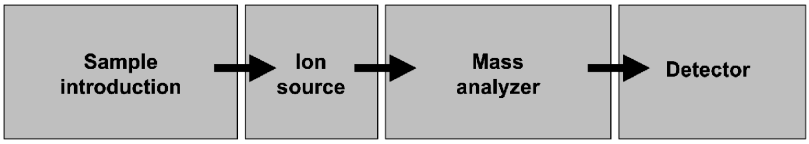

Figure 1 The basic components of a mass spectrometer.

2. THE INSTRUMENT

In the simplest configuration, a mass spectrometer consists of a sample introduction device, an ion source, a mass analyzer, a detector and a data system. These components are most easily conceived as being arranged in a linear array (Figure 1).

Samples are introduced into the ion source in a solid, liquid (in solution or neat) or gaseous state. Proteins are only introduced in solution or as solids. Gas phase ions are made from the sample in the ion source. Spray (ESI, micro- and nano-spray) and LD ionization are the two most important methods for creating gas phase ions from proteins. These gas phase ions are then separated on the basis of their mass/charge (m/z) ratio in the mass analyzer. Quadrupole (Q), quadrupole ion trap (QIT), linear ion trap (LIT), time-of-flight (TOF), ion cyclotron resonance (ICR) and orbitrap analyzers are the most common mass analyzers used in protein research today. Often these analyzers are used in a linked or tandem arrangement in such a way that two analyzers, separated by a gas collision or reaction cell, are assembled in a linear array. The analyzers in a tandem arrangement may have a similar or a different design. Finally the ions are detected. Usually ion currents are measured, often with an electron multiplier, multichannel plate or photomultiplier. Ion counting is sometimes used. The frequency of currents induced in detector plates (image current) is measured in ICR and orbitrap instruments. The data system allows the manipulation of the recorded signals.

3. VACUUM SYSTEMS

In the mass analyzer it is undesirable to have the gas phase analyte ions either deviate from their desired trajectories, or fragment by colliding with gas molecules, unless one deliberately chooses to orchestrate such a collision (as in tandem mass spectrometry or MS/MS). Therefore mass analyzers operate in a vacuum (usually $\leqslant 10^{-5}$ Torr, 1 Torr = 1 mm Hg). Vacuums of this quality are typically generated through two stages of pumping in which a high vacuum pump (ion pump, cryogenic pump, oil diffusion pump or, more commonly on modern instruments, a turbomolecular pump) is connected in series to a rotary mechanical pump.

4. DEFINITIONS

The molecular ion (designated M) represents the intact molecule, and is the precursor of any fragment or adduct ions formed during the ionization process. Typically the charge on the ion is indicated. If the charge results from loss of an electron, attachment of a proton or protons, alkali metal adduction or loss of a proton, the status of the molecular ion is so-indicated (e.g. M^+, MH^+, $(M+6\,H)^{6+}$, MNa^+ and $(M–H)^–$, respectively).

The unit used in mass measurement is the Dalton (Da). This is defined as 1/12th the mass of carbon-12 (^{12}C). Human insulin, for example, has an elemental formula of $C_{254}H_{377}N_{65}O_{75}S_6$ and a molecular weight of 5729.6009 Da for the monoisotopic ($^{12}C_{254}\,^{1}H_{377}\,^{14}N_{65}\,^{16}O_{75}\,^{32}S_6$) species.

Mass spectra are displayed graphically as ion current intensity on the ordinate (y-axis) plotted against the m/z ratio of the ions on the abscissa (x-axis). The ion current intensity can be expressed relative to the most intense signal in the spectrum (percent relative intensity), or alternatively as percentage total ionization (%Σ), which represents the abundance of individual ions expressed as a percentage of the total abundance of all the ions in the spectrum, or as absolute ion intensity (ion counts or ion current).

Integer mass refers to the mass of an element to the nearest whole number. Monoisotopic mass refers to the exact mass of the lightest isotope of each element in the formula. Thus for ^{12}C the integer and monoisotopic masses are, by definition, the same. However, the exact masses of all other elements deviate slightly from their corresponding integer values (Figure 1). This deviation from the integer value is referred to as the *mass defect*, which can be calculated from the monoisotopic mass. Hydrogen, for example, has an integer mass of 1 Da, while the monoisotopic mass of the $^{2}H_1$ atom is 1.00782504 Da. When the naturally occurring hydrogen isotope deuterium ($^{2}H_2$, 2.014101787 Da, 0.015% natural abundance) is taken into account, the average mass of hydrogen is 1.00794 Da; this is also referred to as the chemical mass.

To interpret a spectrum it is essential to know the charge state of the ions. This can usually be determined with certainty, although there are occasions, particularly with low-resolution mass analyzers, when ambiguity arises. The base peak in a mass spectrum is the most intense peak in the spectrum. There is a distinction to be made between profile and centroid data (Figure 2). Profile data is the direct readout from the detector (Figure 2, top panel). In profile data, each signal has a width associated with it, which results from a distribution of imperfect ion measurements. This width is described in terms of resolution (see below), and different analyzers vary in their resolving power. Peaks tend to be symmetrical; however, the asymmetry sometimes evident in profile data can be due to elemental heterogeneity in the ions contributing to the signal, and to imperfections in the performance of the mass analyzer. To simplify data manipulation and presentation (such as for text book presentations), profile data can be converted to a centroid format by arithmetic manipulation. The centroid of a profile peak is defined as the m/z of the profile peak at half the width and at

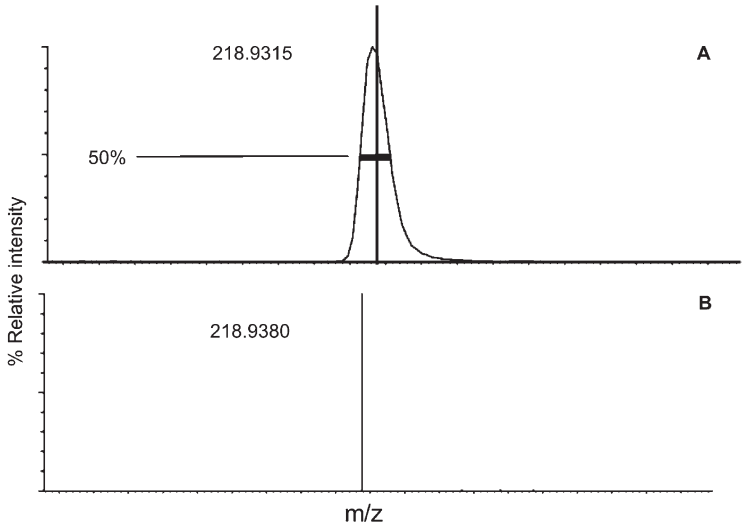

Figure 2 A selected region of the electron ionization mass spectrum of perfluorinated kerosine collected on a time of flight mass spectrometer. Panel A shows a region of the profile spectrum with the apex mass and centroid at half-width/half-height indicated. Note the difference between the centroid mass position and the apex of the profile peak. Panel B shows the centroid mass position of the profile peak from panel A.

half height (Figure 2, lower panel). Thus, the m/z of a centroid peak is not always the same as the m/z of the tallest point of the profile peak.

5. RESOLUTION

Resolution refers to the ability to discriminate between ions of similar m/z. This is a characteristic determined by the mass analyzer but is be influenced by the energy spread of ions emerging from the ion source. There are two methods by which resolution is calculated. The traditional method is defined as $M/\Delta M$ and should be accompanied by notation of the degree of peak separation used when making the calculation (Figure 3). A 10% valley (nadir to zenith ratio) is most commonly used while a 50% valley is often used for TOF analyzers (early TOF analyzers produced spectra with broad "feet"). While this method of calculating resolution is referred to as the $M/\Delta M$ method, it should more correctly be referred to as $(m/z)/(\Delta m/z)$ method, because the m/z values are used in the calculations. There are three general levels of resolution. Low resolution usually implies unit resolution in the mass range of interest, as in Figure 3, for example, where m/z 906.5 is separated from 907.7 with a 10% valley. Medium resolution implies a resolution between 4,000 and 10,000. High resolution implies a resolution of 10,000 or greater.

Conventional quadrupole and QIT analyzers are unit resolution instruments, although the new generation instruments, including LIT instruments, are capable

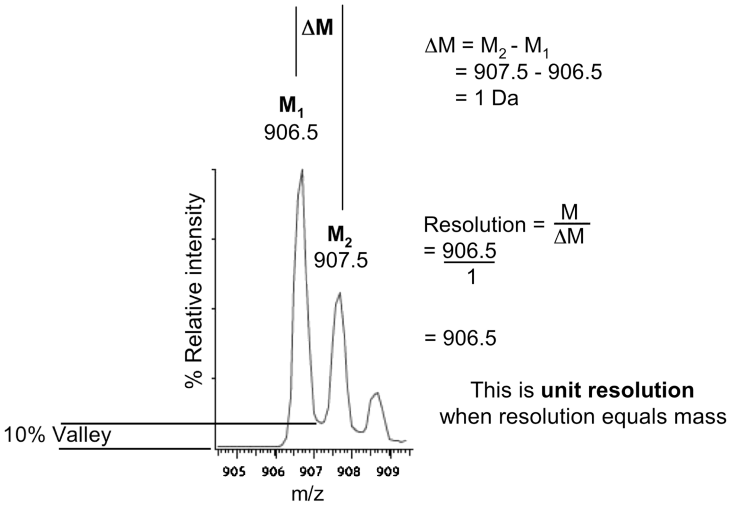

Figure 3 M/ΔM method for calculating resolution. The difference (DM) between the monoisotopic peak at 906.5 and the $^{13}C_1$ peak at 907.5 is 1 Da. Thus, 906.5 Da divided by 1 Da equals 906.5, which is the resolution (M/ΔM method) at this point in the mass spectrum. Unit resolution is the term used when resolution equals the mass. This signal, from an ammonium adduct of a polypropylene glycol component, was collected on an electrospray triple quadrupole instrument.

of higher resolution. Double focusing magnetic sector instruments (magnetic and electrostatic analyzers in series) are high-resolution instruments, older linear TOF analyzers are low-resolution instruments, but when equipped with a reflector, and particularly with time-lagged focusing, TOF analyzers are capable of high-resolution measurements. The orbitrap and ICR cells are capable of extraordinarily high resolution.

An example of the need for high resolution emerged during the analysis of the first moon rock samples brought back to earth from the Apollo mission in 1969. At this time there was interest in determining if these samples contained organic molecules indicative of life. Several laboratories prepared extracts of the samples and used mass spectrometry to search for amino acids, porphyrins and other biochemicals in the samples. One of the few findings was the presence of relatively large amounts of CO in the samples, but recognition of CO required sufficient resolution to separate CO from N_2.

$^{12}C^{16}O$	Nominal mass 28	Monoisotopic mass 27.9949
$^{14}N_2$	Nominal mass 28	Monoisotopic mass 28.0061

The resolution required for the separation of CO and N_2 is $\geqslant 28/0.0112 =$ 2,500. This resolution could not be obtained on quadrupole mass analyzers, and the discovery of the relatively large amounts of CO in the samples was made by the group that used a magnetic sector instrument with a much higher resolution (B. Halpern, personal communication) [9].

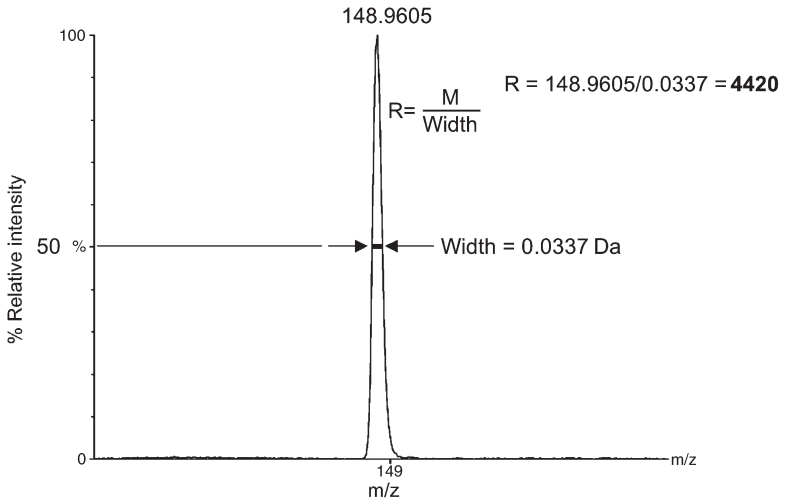

Figure 4 Full width at half height method (FWHM) for calculating resolution. The width of this peak at *m/z* 148.9605 at half height is 0.0337 Da. Thus, the FWHM resolution is calculated as 148.9605 divided by 0.0337 (= 4420). This signal is an EI fragment ion from a phthalate collected on a time of flight mass spectrometer connected to gas chromatograph.

The other method for calculating resolution was developed for spectra obtained on TOF analyzers, but has since become the more commonly used approach. Termed the "full width at half height method" (FWHM), this calculation can be made from single ions (Figure 4).

The M/ΔM and FWHM approaches for calculating resolution produce widely differing numerical values from the same data (Figure 5), hence the requirement for method stipulation when resolution values are cited.

6. MASS ACCURACY

This refers to the precision with which the m/z value of a peak can be assigned. The precision of this assignment is a characteristic of the mass analyzer and is influenced by the scan-to-scan variation in the m/z assignment of the peak (i.e. reproducibility of the scan by the mass analyzer). The deviation between a calculated mass and the experimentally measured mass is expressed in milli Da (mDa) or parts per million: ppm = (calculated mass−measured mass) $\times$ 10^6/ calculated mass.

A reasonable rule of thumb is that, with the current technology and ions up to about m/z 4,000, the best mass measurement accuracies are in the low ppm range (1–10).

All mass spectrometers must be calibrated. For external calibration the mass analyzer is calibrated across the mass range of interest with a standard that may be a single compound but more commonly is a mixture of compounds. The unknown(s) are then analyzed and the m/z values of detected ions are assigned

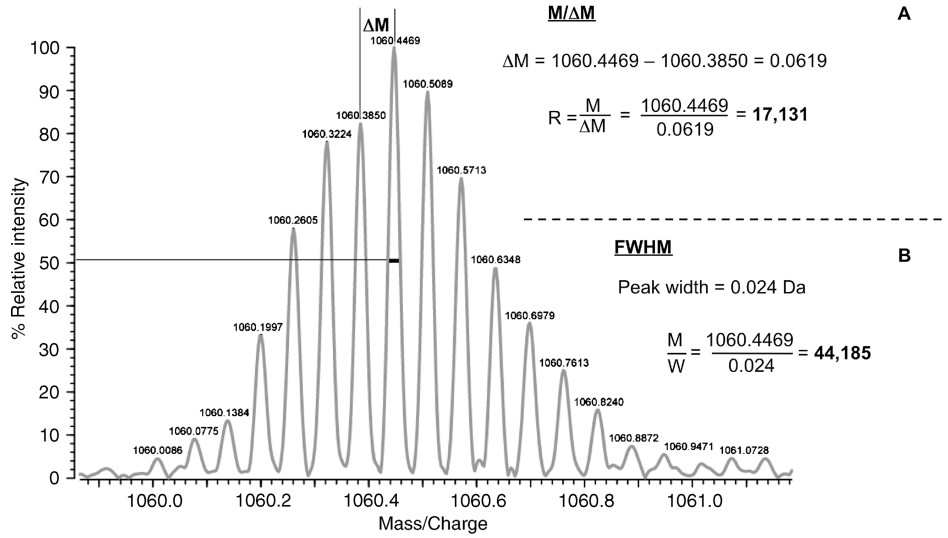

Figure 5 Comparison of M/ΔM and FWHM methods for calculating resolution. See Figures 3 and 4 for a description of the M/ΔM and FWHM methods, respectively. Notice the large difference in the numerical values for resolution calculated from the same data. This spectrum is the 16 charge state electrospray ion of horse myoglobin recorded with a Fourier transform mass spectrometer.

using the calibration established with the standard. While external calibration is easier to perform, the most precise measurements are made with internal calibration in which the standard and the unknown are present in the source simultaneously. After collection of the spectra the signals from the standard are assigned, and then the assignments for the unknown signals are made by inter- or extra-polation. In the case of internal calibration the difficulty arises in obtaining a good balance for the ion intensities from the calibrant and the unknown(s), and requires the availability of suitable compounds for use as internal calibrants.

Calibrants commonly used for electron impact and chemical ionization include perfluorinated kerosene (commonly referred to as heptacosa or FC-43) which are available as a range of boiling point mixtures (the thermal stability and negative mass defect of fluorinated calibrants is an advantage). Cesium iodide (CsI) and mixtures of CsI and RbI are often used as calibrants for fast atom bombardment (FAB) and liquid secondary ionization (LSIMS) sources, and sometimes for ESI and laser desorption (LD) sources. A variety of peptides, proteins and polypropylene glycols ($[CH_2CH_2CH_2O]_n$) are used as calibrants for ESI and matrix-assisted LD (MALDI).

7. ISOTOPES

Most elements have naturally occurring stable isotopes; this can be both a bane and a blessing. The bane comes from the added complexity they contribute

to the spectra; the blessing comes from the help they provide for determination of the chemical formula and the charge state of an ion (see below). In organic and biochemical applications, the appearance and interpretation of resolved mass spectra is complicated by the naturally occurring isotopes of C, H, O, N, P and S. Of these, the naturally occurring carbon-13 (^{13}C) isotope adds the most complexity because of the prevalence of carbon and the fact that carbon-13 accounts for about 1.1% of the carbon on earth. If an ion contains 10 carbon atoms, then the signal corresponding to the $^{12}C_9{}^{13}C_1$ component will have a relative intensity of $10 \times 1.1\% = 11\%$ compared to the $^{12}C_{10}$ component. As illustrated in Figure 6, as the number of carbon atoms in an ion increases, so does the relative intensity of the $^{13}C_1$ component (and $^{13}C_2$, etc.) until it exceeds the intensity of the all-^{12}C component. The $^{13}C_1$, $^{13}C_2$, etc. containing peaks are referred to as isotopomers. The masses and abundances of the common biological elements and their common isotopes are shown in Figure 7.

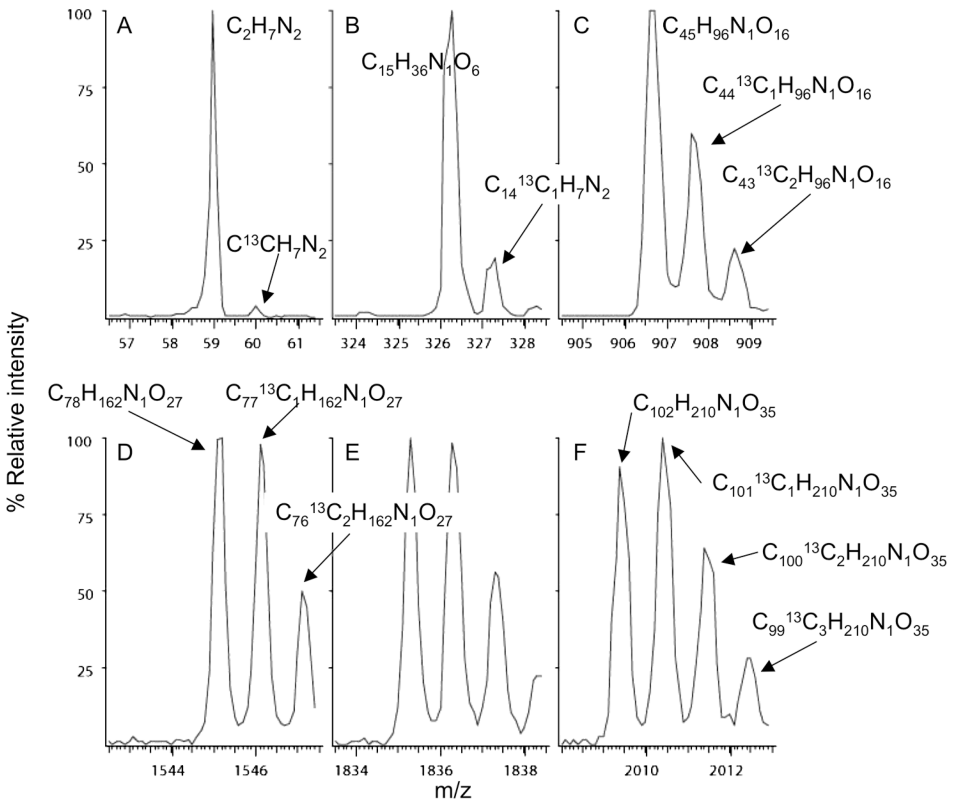

Figure 6 Molecular ion regions of the ammoniated adduct ions formed by electrospray from acetonitrile (A) and polypropylene glycol components (B–F). Note the increased relative intensity of the $^{13}C_1$ isotopomers with respect to carbon content. Panel E is not labeled for increased clarity.

Element	Integer mass (Da)	Monoisotopic mass (Da)	Isotopes (abundance)	Average mass (Da)
C	12	12.000	^{12}C 100% ^{13}C 1.08%	12.0110
H	1	1.00782504	^{1}H 100% ^{2}H 0.016%	1.00794
N	14	14.00307	^{14}N 100% ^{15}N 0.4%	14.00674
O	16	15.99491464	^{16}O 100% ^{17}O 0.04% ^{18}O 0.2%	15.99940
P	31	30.9737634	^{31}P 100%	30.9737634
S	32	31.9720718	^{32}S 100% ^{33}S 0.8% ^{34}S 4.4%	32.069

Figure 7 Integer, monoisotopic and average (chemical) masses of the elements found in proteins.

8. RECONCILING THEORETICAL AND MEASURED MASSES

When the mass of a molecule is calculated (theoretical mass) for comparison with a measured mass, the resolution in the mass spectrum dictates which of the elemental masses (monoisotopic or chemical) should be used. In Figure 8, the comparison should be made with calculations based on monoistopic masses with the resolved data (right panel), and with average (chemical) masses with the unresolved data (left panel). The calculation of the molecular weight of a polymer is accomplished from the sum of the residue masses of the monomer units, to which the mass of the end groups is added. In the case of peptides and proteins, as already stated, the amino acid masses are unique, with the exception of leucine and isoleucine (Table 1), making them particularly amenable to characterization on the basis of their mass.

9. CHARGE STATE ASSIGNMENT

Charge state assignment is essential for the interpretation of any mass spectrum. Singly charged ions of organic molecules are characterized by a 1 Da separation between the ^{13}C-containing isotopomers (ΔM), doubly charged ions are characterized by 0.5 Da separation, triply charged by 0.33 Da separation, etc. Because the charge state of an ion is the inverse of the separation between the ^{13}C-isotopomers (charge state $= 1/\Delta$M), the charge state can be calculated from the data in a mass spectrum so long as there is sufficient resolution of the

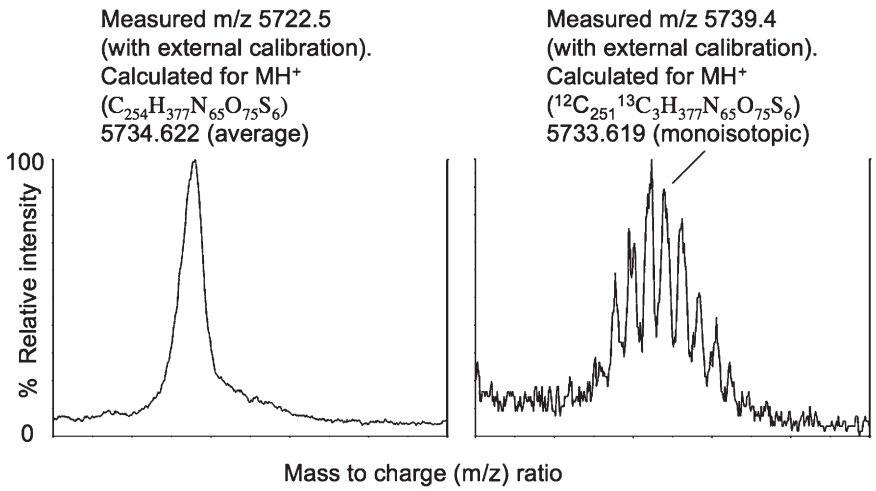

Figure 8 Comparison of insulin mass spectra collected under non-resolving and resolving conditions. The figure shows the molecular ion region of bovine insulin collected on a MALDI-TOF instrument at low resolution (left panel, linear mode with time-lagged focusing) and at a resolution of about 5,000 (FWHM, reflectron mode with time-lagged focusing, right panel). Both of these spectra are the average from 500 laser shots at a spot containing 5 pmol of bovine insulin and α-cyano-4-hydroxy-cinnamic acid matrix.

isotopomer ions. For example, the ion in Figure 3 has a charge state of 1 (1/1), the ions in Figure 5 have a charge state of 16 (1/0.0619 = 16.2), all the ions depicted in Figure 5 have a charge state of 1 (1/1), and the insulin ion in Figure 8 (right panel) is singly charged (1/1), but the charge state cannot be determined from the unresolved insulin ion (Figure 8, left panel).

10. THE NEED FOR CHROMATOGRAPHY

The idea of eliminating chromatography from the workflow of complex sample analysis, thus limiting manipulation of the sample and shortening analysis time, has been repeatedly revisited. In 1966 chemical ionization (CI) was discovered, and at the time was thought to have promise in this regard [10]. The reason for this expectation was the hope that the simple spectra produced during CI would have sufficient inherent specificity for the identification and quantification of targeted compounds in complex extracts from direct analysis by solid probe techniques. For complex samples this hope did not materialize except in a few isolated circumstances [11,12]. The subsequent development of tandem mass spectrometry revitalized this hope, and the more recent development of MALDI-TOF has had the same effect. Nevertheless, complex samples almost invariably require chromatography, and the time delay and extra complications imposed appear inescapable facts of life.

The direct coupling of LC to MS is more difficult than GC/MS coupling because of the gas load created by vaporization of the LC effluent (e.g. 100 µl/min

of water will create 124.4 ml/min of vapor at STP). Despite this problem there have been several generations of LC-MS interfaces. Today, for peptides and proteins LC-MS is virtually the exclusive domain of ESI [13]. However, because of limitations imposed by ESI, there are restrictions on the type of eluants that can be used for LC during LC-MS. Because ESI is sensitive to involatile inorganic salts (the inorganic salts tend to sequester the ion current and strip the charge from the organic analytes of interest), eluants containing common biochemical buffers such as phosphate, sulfate, Tris, sodium and potassium are poorly tolerated. Reverse phase LC using aqueous eluants mixed with organic modifier (methanol or acetonitrile) are well tolerated, with dilute acid for the positive ion mode (commonly 0.1% formic or acetic acids because trifluoroacetic acid tends to suppress the ion signal) and appropriate pH adjustment for the negative ion mode (ammonium acetate, pH 5).

Multidimensional chromatography is required for particularly complex samples. The combination of ion exchange and reverse phase, developed by Yates and colleagues [14], has been an important development because of the unidimensional design and the high capacity of both chromatographic modalities. The disadvantage of this method is the relatively low resolution of the ion exchange step that results in the appearance of an analyte in more than one ion exchange fraction. Other multidimensional techniques, such as chromatofoccusing combined with reverse phase chromatography in a two-dimensional (2D) format, have also been used, but the low resolution of chromatofocusing has limited the applicability of this approach. There remains a need for a robust, high capacity, high resolution, mass spectrometrically compatible, orthogonal separation modality that can be conveniently used in combination with reverse phase chromatography. Hydrophilic interaction chromatography (HILIC) meets some of these requirements, and although the newer resins appear to have adequately stable behavior and good resolving power, their capacity has yet to be thoroughly tested.

11. THE MYTH OF DEFINING ELEMENTAL COMPOSITIONS

Because all elements have a unique mass, it has long been proposed that if the m/z of an ion is measured with sufficient accuracy, an elemental composition can be determined from first principles without additional information. However, in practice this is only fulfilled at relatively low m/z and with the best available mass measurement accuracies (low ppm range; Figure 9). At higher m/z there is an exponentially increasing number of elemental possibilities that can account for the observed mass of an ion. Therefore, to restrict the number of acceptable elemental combinations, an exponentially increasing mass measurement accuracy would be required, and this is not provided by any of the available mass analyzers. Conversely, an accurate mass measurement can always be used to substantiate a hypothesized elemental formula, regardless of the molecular weight.

At the current level of technological development the following rules of thumb are worthy of note. Mass measurement accuracies of less than 10 ppm are

	Mass measurement accuracy			
Ion (m/z)	< **2ppm**	< 5ppm	< 10ppm	< 20ppm
100.0258	CH_2N_5O	CH_2N_5O	CH_2N_5O	CH_2N_5O H_6NO_5 $C_3H_4N_2O_2$
275.2689	$C_{13}H_{33}N_5O$	$C_{13}H_{33}N_5O$ $C_{15}H_{35}N_2O_2$	$C_{13}H_{33}N_5O$ $C_{15}H_{35}N_2O_2$	**Five possibilities**
773.5624	$C_{48}H_{76}N_3O_3P$ And 20 others!!	**Fifty three possibilities**	**One hundred possibilities**	**Too many to count!**

Figure 9 The power of exact mass. The table lists the combinations of carbon, hydrogen, nitrogen, oxygen, phosphorous and sulfur that can account for the three listed ions at four different mass measurement accuracies. The elemental compositions are restricted to 0–500 for carbon, 0–1,000 for hydrogen, 0–6 for nitrogen and oxygen, 0–3 for phosphorous and 0–4 for sulfur.

generally accepted as adequate for reconciling measured m/z signals with calculations based on molecular formulas, particularly with molecular weights below 2 kDa. Mass measurement accuracies better than 1 ppm are rarely achieved on a routine basis, although very recent results with the orbitrap instrument suggest such measurements may become more common in the future (Joshua Coon, unpublished observations). Measurements by Fourier transform mass spectrometry (FTMS) typically have less than 3 ppm accuracy. New generation TOF mass spectrometers can now produce 2–5 ppm accuracy. The orbitrap mass spectrometer can produce low ppm accuracies. Quadrupole and QIT mass measurement accuracies are generally no better than 20 ppm.

12. DESORPTION IONIZATION: LASER DESORPTION

Today LD is the most important desorption ionization method in use, and the acronym MALDI is used to denote when LD is used in conjunction with a matrix to assist the ionization process. Work in the 1970–1980s, particularly that of Ron Macfarlane with ^{252}Cf-desorption from a solid surface, and of Michael Barber and colleagues with atom (and subsequently ion) beam desorption from a liquid surface, provided the inspiration for others to search for improved methods for the efficient ionization of large molecules [4,5,15,16]. LD had been under investigation since the 1980s also, but crucial observations by Tanaka and Karas and Hillenkamp who obtained strong ion currents for proteins when they were

co-crystallized with a small organic molecule which absorbed energy in the region of the laser light source, ushered in the MALDI era [6,7]. This technique is usually used in conjunction with a TOF mass analyzer because of the compatibility of the pulsed ion source and the TOF analyzer (Figure 10). Probably the most gentle mode of ionization available today, it is used for analysis of a wide range of compounds from low-mass materials to the analysis of proteins with molecular weights >100 kDa. The ionization process can tolerate inorganic salts and other additives commonly used in biochemical preparations (except sodium dodecyl sulfate, SDS). The process can be extraordinarily sensitive (fmol–pmol required), but the high chemical background derived from the matrix can be a problem in the low m/z range ($m/z<1{,}000$).

LDMS spectra are generally characterized by intense singly charged ions. The mechanism of ion formation is probably complex and it is likely that there is more than one process involved. A simple analogy can be made with the CI and perhaps also the FAB ionization processes. Ion formation in CI and FAB has been thoroughly investigated. It is generally thought to involve a reaction between a gas phase ion (a proton donor derived from the reagent gas or liquid matrix) and a gas phase molecule (the analyte). A similar reaction may take place during LDMS. Immediately following adsorption of the laser pulse a dense plume of gas phase material is generated. Desorbed analyte molecules react in the gas phase with proton donors that are formed upon molecular disintegration of the organic molecules (matrix and sample) in the immediate vicinity of the point of laser impact. Such a gas phase ion-molecule reaction would have favorable rate constants and would predominately result in the formation of singly protonated analyte molecules.

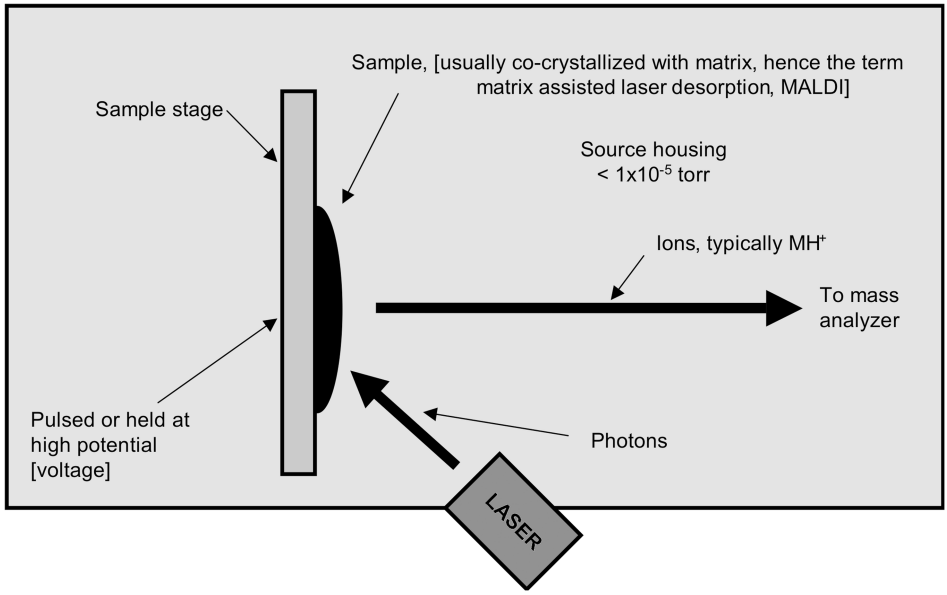

Figure 10 Simplified schematic representation of a laser desorption ion source.

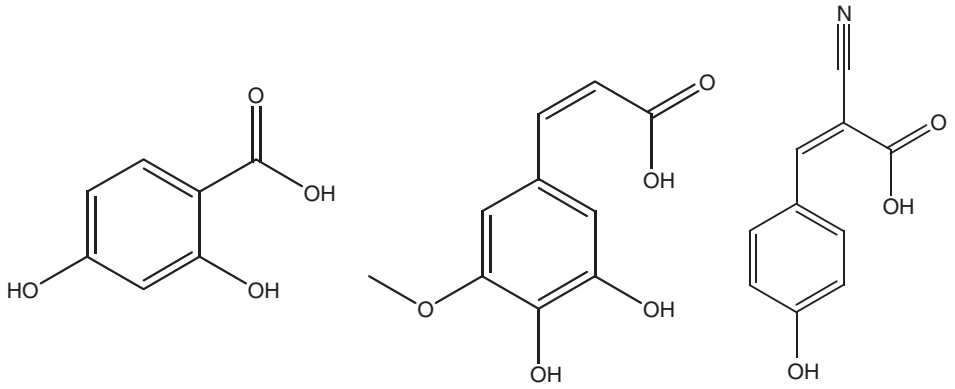

Figure 11 Some commonly used MALDI matrices: 2,5-dihydroxybenzoic acid (left, DHB, used for peptides, carbohydrates and glycolipids), α-cyano-4-hydroxy-cinnamic acid (center, commonly referred to as "alpha", used for peptides) and 4-hydroxy-3,5-dimethoxy-cinnamic acid (right, sinapinic acid or sinapic acid, used for proteins).

The art in MALDI analysis lies in the preparation and co-crystallization of the matrix and sample. A number of matrices have been successfully used. Those favored for peptides and proteins are simple aromatic organic acids that absorb at or near the wavelength of the laser pulse. Those most commonly used are shown in Figure 11. The accuracy of molecular weight measurements of proteins by MALDI-TOF is $<0.1\%$ of the mass.

13. SPRAY IONIZATION: ELECTROSPRAY IONIZATION

This phenomenon was originally observed by Malcolm Dole, but rediscovered by John Fenn and colleagues at Yale in the early 1980s, work for which Fenn was awarded the 2002 Nobel Prize in Chemistry [17–21]. Alexandrov and colleagues in Russia independently described the phenomena, but their contribution is generally not widely acknowledged in the West [22]. The process works by forcing a solution of the analyte through a capillary to which a voltage is applied (Figure 12). For flow rates above several micro liters per minute (typically referred to as electrospray), a coaxial gas is applied to aid in the formation of a spray from the tip of the capillary. For flow rates less than several micro liters per minute (typically referred to as micro- or nano-spray), no gas is needed as a spray develops naturally due to the high-voltage applied. The emerging droplets of the spray are charged, lending the name to the technique. On encountering heat and frequently an opposing flow of gas (bath gas), the solvent in the droplets begins to evaporate. As the droplet size decreases due to this evaporation, the prevailing theory is that the charge density in the droplet increases and eventually naked ions are ejected as a consequence of charge repulsion. Molecules emerge with one or more proton adducts; for example, MH^+ in the positive mode (Figure 13A), $(M–H)^-$ in the negative mode (Figure 13B); and larger molecules emerge with

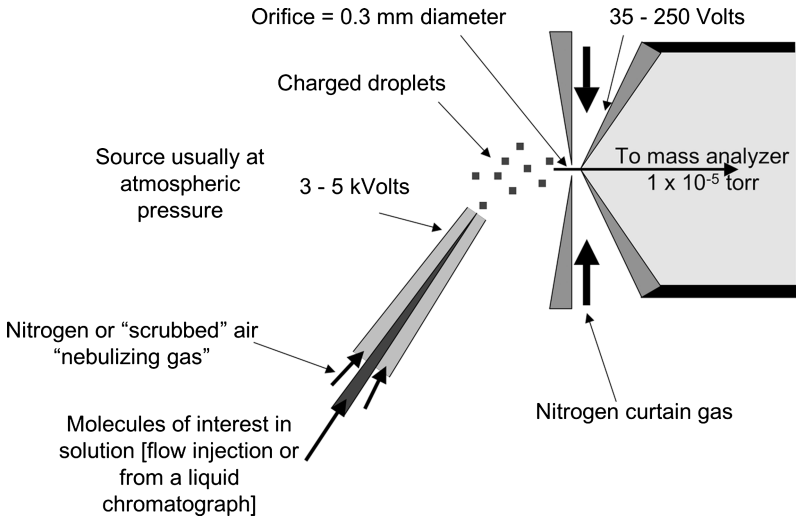

Figure 12 Simplified schematic representation of an electrospray ionization source. Adapted from the Ionspray™ design of Applied Biosystems/MDS Sciex.

many charges (Figure 13C). These ions then enter the high vacuum of the mass spectrometer through varied inlet technologies and geometries depending on the type of analyzer the ESI source design.

This technique is extraordinarily effective at producing gas phase ions from a wide range of involatile molecules. Thermal stability is not a requirement, but the process is intolerant of involatile inorganic ions, and SDS. The ionization mass range is presumably unlimited, certainly >100 kDa, but because the observed m/z value of ions from large molecules (e.g. proteins) is almost always less than 4,000 (often less than 2,500) due to the multiple charge states, ESI is frequently attached to a mass analyzer with a limited mass range (e.g. quadrupole and ion trap instruments). The production of multiply charged ions from macromolecules such as proteins (Figure 13C) may at first glance appear to complicate the interpretation of the spectra [23]. However, a number of arithmetic algorithms have been developed for deconvolution of the mass spectra into true molecular weight spectra (Figure 13D). One easy way to visualize the process is to calculate the molecular weights for each ion in the spectrum across a range of charge states (Figure 14). Ions of differing charge state originating from the same molecule then emerge as matching molecular weights across the diagonal of the display. Ions that are not part of the series do not fit the matching molecular weight at any charge state.

The accuracy of molecular weight measurements by ESI is astonishingly good, and for proteins is usually quoted as less than $\pm 0.01\%$ of the mass. A celebrated example of the precision of this mass assignment emerged shortly following the use of ESI for the analysis of proteins. The molecular weight of myoglobin (153 residue protein) calculated from the X-ray structure is 16,950.5 Da. The molecular weight measured by ESI was found unequivocably to be 16,951.5 Da [24]. Apparently residue 122 was mis-assigned in the X-ray

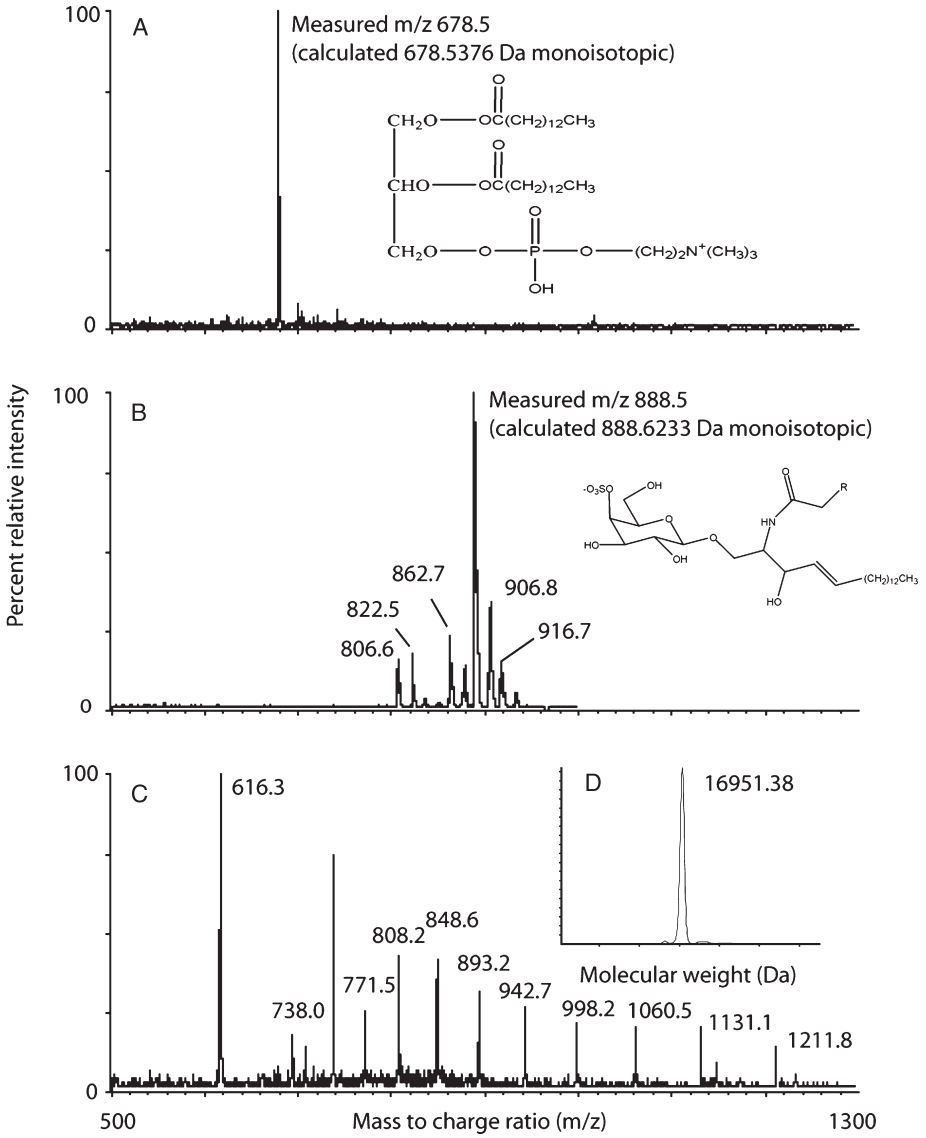

Figure 13 Representative ESI mass spectra collected on a quadrupole mass spectrometer: (A) dimyristoyl phosphatidyl choline, positive ion mode, (B) bovine brain sulfatides, negative ion mode, (C) bovine heart myoglobin, positive ion mode and (D) molecular weight spectrum derived from the mass spectrum shown in (C).

structure as asparagine rather than aspartic acid (–COOH = 45 Da, $–CONH_2$ = 44 Da). This mis-assignment may not be important for the function of myoglobin, but in biology there are many examples where 1 Da conversion of the free carboxyl form of a peptide hormone to the amide form has a major effect on the biological potency of the molecule.

Observed	Ion charge state (12-24)												
ions (m/z)	12	13	14	15	16	17	18	19	20	21	22	23	24
1305.00	15647.9	**16951.9**	18255.9	19559.9	20863.9	22167.9	23471.9	24775.9	26079.8	27383.8	28687.8	29991.8	31295.8
1211.80	14529.5	15740.3	**16951.1**	18161.9	19372.7	20583.5	21794.3	23005.1	24215.8	25426.6	26637.4	27848.2	29059.0
1131.10	13561.1	14691.2	15821.3	**16951.4**	18081.5	19211.6	20341.7	21471.8	22601.8	23731.9	24862.0	25992.1	27122.2
1060.50	12713.9	13773.4	14832.9	15892.4	**16951.9**	18011.4	19070.9	20130.4	21189.8	22249.3	23308.8	24368.3	25427.8
998.20	11966.3	12963.5	13960.7	14957.9	15955.1	**16952.3**	17949.5	18946.7	19943.8	20941.0	21938.2	22935.4	23932.6
942.70	11300.3	12242.0	13183.7	14125.4	15067.1	16008.8	**16950.5**	17892.2	18833.8	19775.5	20717.2	21658.9	22600.6
893.20	893.2	893.2	12490.7	13382.9	14275.1	15167.3	16059.5	**16951.7**	17843.8	18736.0	19628.2	20520.4	21412.6
848.60	10171.1	11018.7	11866.3	12713.9	13561.5	14409.1	15256.7	16104.3	**16951.8**	17799.4	18647.0	19494.6	20342.2
808.20	9686.3	10493.5	11300.7	12107.9	12915.1	13722.3	14529.5	15336.7	16143.8	**16951.0**	17758.2	18565.4	19372.6
771.50	9245.9	10016.4	10786.9	11557.4	12327.9	13098.4	13868.9	14639.4	15409.8	16180.3	**16950.8**	17721.3	18491.8
738.00	8843.9	9580.9	10317.9	11054.9	11791.9	12528.9	13265.9	14002.9	14739.8	15476.8	16213.8	**16950.8**	17687.8

Figure 14 Interpretation of the spectrum of multiply charged ions derived from the ESI spectrum of myoglobin shown in Figure 13C. The observed ions from the mass spectrum (Figure 13C) are listed in the left-hand column. The body of the table is a listing of molecular weights calculated for each ion with charge states 12–24 using the formulae molecular weight = (m/z × charge state)−mass of the charging species, when the charging species is gained, species H, mass 1.0079 Da. The correspondence shown in bold font across the diagonal reveals the matching calculations which show the observed ions have charge states ranging from 13 (m/z 1305.0) to 23 (m/z 738.0), and the average of the calculations (16951.38) is within experimental error (+/− 0.01% for measurements of this type made on quadrupole mass spectrometers at unit resolution) of the molecular weight calculated from the protein sequence (16951.5 Da).

14. MASS ANALYZERS

Gas phase ions can be separated on the basis of their m/z ratio using the physical principles that define the motion of ions within magnetic or electromagnetic fields, or the time taken to drift through a field-free space following acceleration. These techniques spread the ions in time and/or space, thus allowing their independent detection. Mass analyzers are usually grouped according to the physical principles by which ions of different m/z are separated, for example magnetic sector, TOF, ICR, etc. Another way to group mass analyzers is according to their mode of operation with respect to how the ion beam is generated; thus, there are instruments that have a continuous mode of operation (so-called scanning instruments; magnetic sectors, quadrupoles), others with a pulsed mode of operation (TOF), and yet others with an ion trapping mode (QITs, ICR cells, orbitraps). Yet another way to group mass analyzers is with respect to how the ion beam is measured, either as integrating or non-integrating instruments. All mass analyzers have advantages and disadvantages, and there is no single instrument that is ideal for all applications and experiments. The nature of the problem and the instruments available in the laboratory dictate the mass analyzer that will be used for any given experiment.

The distinction between integrating and non-integrating analyzers should be dealt with in more detail. At any point in time, a non-integrating mass analyzer (e.g. a quadrupole analyzer) focuses only a small portion of the ion beam at the detector, and the remainder of the ion beam is discarded. However, integrating mass analyzers (e.g. TOF and ICR cells) detect essentially the entire ion beam. Thus with pulsed beam ion sources, integrating analyzers have an advantage over their non-integrating counterparts. With continuous beam ion sources, the

advantage of integrating instruments is diminished unless the duty cycle of the analyzer is such that a major portion of the ion beam is accepted. The disadvantage for non-integrating instruments can be offset, at least partially, for targeted compound analysis, by focusing on a specific ion or ions. In the MS mode this is referred to as selected ion monitoring (SIM), and in the MS/MS mode this is referred to as selected reaction monitoring (SRM, parent ion to product ion transition or reaction) or multiple reaction monitoring (MRM). Thus with SIM, SRM and MRM, the ion- or reaction-specific traces or chromatograms are collected in lieu of complete mass spectra. These modes of data collection are commonly used with chromatographic sample introduction for quantitative analyses.

15. TIME-OF-FLIGHT MASS SPECTROMETERS

The method of ion separation by these instruments is most easily visualized by imagining a collection of ions aligned on a plane in a vacuum (Figure 15). A plate positioned behind the ions is then charged with a high electrical potential of the same polarity. The ions are repelled away from the plate. The force of repulsion is dependent on the charge of the ion and not the mass. So, two singly charged ions of different masses will feel the same repulsive force, however, the lower inertia of the less massive ion will translate into an increased velocity away from the plate. After passing through some grids that shield the ions from the force fields, they then drift through a field-free region until they strike the detector. The ions with low m/z strike the detector first, followed by ions of higher m/z. The time taken for the ions to traverse the drift tube is recorded. This time depends on mass, the number of charges, and the acceleration potential. The flight time (t)

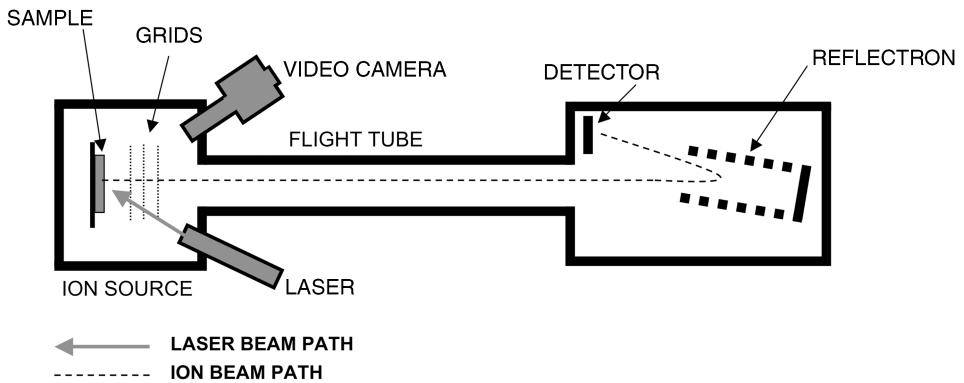

Figure 15 Schematic representation of a MALDI-TOF instrument equipped with a reflectron. The sample is co-crystallized with matrix (see Figure 10). The function of the grids is to shield ions in the flight tube from the voltages associated with the source. In this way, the flight tube is "field free", allowing the ions to drift toward the detector after their initial acceleration. Adapted from an Applied Biosystems instrument design.

can be calculated from the equation:

$$t = d/\sqrt{2U} \cdot \sqrt{m/q},$$

where d is the distance traveled, U the voltage used to repel the ion into the field-free drift tube, m the mass of the ion and q the charge on the ion.

Typical instrument designs have fight tubes of 1 m or so in length and use repelling (usually referred to as accelerating) voltages of around 20 kV. So, for example, the singly charged ions of mass 23 (Na^+), 100, 1,000 and 4,000 Da in a 1-m flight path with 20 kV accelerating voltage, experience flight times of 2.44, 5.09, 16.10 and 32.19 μs, respectively.

Of course it is impossible to perfectly align a collection of ions on a plane in the gas phase. However, laser pulses, when directed at samples embedded in a matrix on a flat surface, produce packets of ions with relatively small dispersion in energy and space. Hence the combination of LD and TOF analyzers is a compatible configuration. In addition, orthogonal extraction of ions from a continuous ion beam by the use of a repeller (or pusher) operated at high voltage and frequency, effectively produces packets of ions also with small energy spread. Thus these analyzers are also used in combination with continuous beam ion sources.

The performance of TOF analyzers is improved with the use of time-lagged-focusing of the ions in the ion source. In the case of laser desorption, this can be visualized by imagining the packet or plume of gas phase ions that result from the impact of a laser pulse as a cloud. With the repelling voltage on continuously, the ions will move down the flight tube as a cloud immediately after formation, thus limiting the separation (resolution) of ions of different m/z. If, however, the repelling voltage is applied a small interval after the impact of the laser pulse, those ions in the cloud closest to the repelling plate will experience a slightly stronger repulsive force than those ions on the distant side of the cloud. The effect will be to narrow the width of the cloud and change its shape into a pancake. Thus the energy and spatial dispersion of ions will be reduced, resulting in improved separation between ions of similar m/z as they travel down the flight tube.

The performance of these instruments is also improved with the use of a reflectron, otherwise known as a Mamyrin ring after the inventor Boris Mamryin (Figure 15), which is in effect an electrostatic mirror. These devices serve to correct, during flight, for small differences in the velocity spread of ions with the same m/z, and thus improve resolution. The reflector is positioned toward the end of the drift tube. Ions with higher velocity penetrate deeper into the mirror than those with the same m/z but lower velocity. On emerging from the mirror, ions with the same m/z have less spatial separation and are more clearly separated from ions with a slightly different m/z. Thus an instrument may be equipped with two detectors, one positioned at the end of the flight tube for use when the reflector is not used (linear mode of operation), and the other positioned off-axis to collect ions as they emerge from the reflector (Figure 15). On commercial TOF instruments the reflectors are effective at separating the

carbon isotope clusters in molecules out to about m/z 6,000. An example of insulin MALDI-TOF spectra collected both with and without the use of a reflector are shown in Figure 8. Most modern TOF analyzers are equipped with both a reflector and time-lagged-focusing to improve resolution.

16. LINEAR QUADRUPOLE MASS FILTERS

The operation of these instruments (and the QITs and LITs described below) is based on the motion of ions in modulated electric fields, a combination of radio frequency (RF) and direct current (DC) fields. Wolfgang Paul and Hans Dehmelt were awarded the Nobel Prize in Physics in 1989 for their independent work developing the theory behind their operation and performance, and for constructing the first instruments. In the late 1950s, Robert Finnigan saw the practical potential of these devices and was the first to commercialize their construction. This effort was aided by the growing need for robust methods to monitor environmental contamination with industrial and other pollutants, and it coincided with the virtually simultaneous development of combined GC/MS. At this time, magnetic sector instruments were the most common type of mass analyzer in use. Quadrupoles appeared more suited to GC coupling because they operated at higher pressures than magnetic sectors and, because they were not hampered with the difficulties inherent to rapidly changing a magnetic field, they could be scanned at rates more compatible with the 10–20 s GC peak widths common on the packed columns that were then in use.

Linear quadrupole mass filters, or commonly, quadrupole mass filters or ''quadrupoles'', are not to be confused with their three-dimensional (3D) or cubic counterparts (the QITs discussed in the next section). The filter consists of an assembly of four symmetrically arranged rods to which RF and DC voltages are supplied (Figure 16). Theoretically, rods with hyperbolic cylindrical cross-sections perform better, although for convenient fabrication most are constructed with carefully machined rods with a circular cross section. The rods are positioned with identical diagonal distances between them. With the z-axis running longitudinally down the center of the assembly, and the x–y axes perpendicular to the rods, ions are injected along the z-axis. The motion of ions in the x and y planes, but not in the z-direction, is influenced by the superimposed RF and DC fields. This motion is described by the Matthieu equations [25]. Optimal performance of the filter depends on precise and stable DC and RF fields along the entire length of the rod assembly. The injected ions undergo transverse oscillations in the x–y plane, with frequencies that depend on their m/z value and with oscillations about the z-axis that depend on the magnitude of the applied RF and DC fields. With proper selection of RF and DC, ions of a given m/z will have relatively small oscillations about the z-axis, and they will pass through the assembly without striking either the rods or the walls of the device, and impinge upon the detector positioned at the end of the assembly; ions with other m/z values will have larger oscillations about the z-axis that increase in amplitude until they collide with the rods or the walls of the device, thus being neutralized

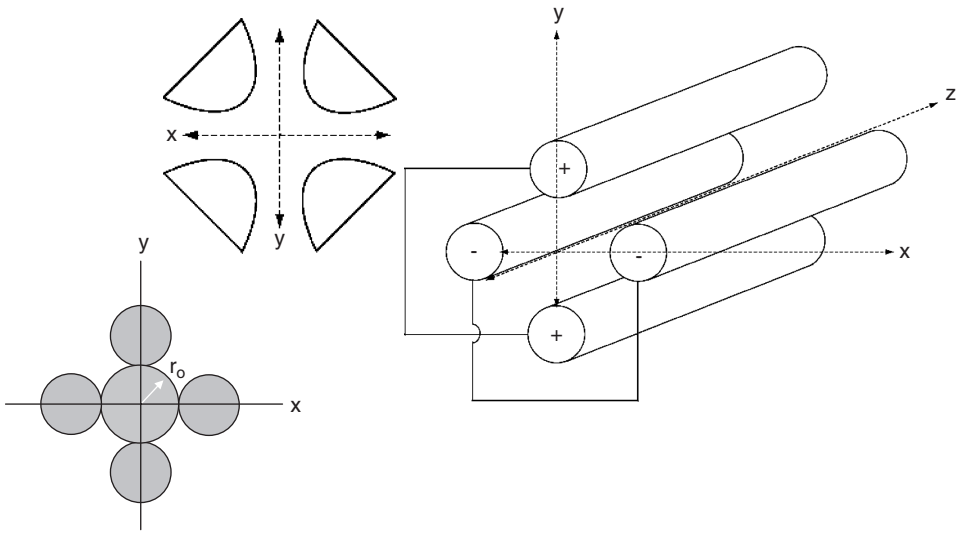

Figure 16 Schematic representation of a set of quadrupole rods. The *x*, *y* and *z* axes are labeled. Ions injected into the assembly along the *z*-axis undergo oscillations of varying magnitude in the *x* and *y* planes as they travel down the length of the rods. Two cross-section diagrams are shown, one with circular rods, the other with more efficient, but harder to manufacture, hyperbolic rods.

and removed from the ion beam. A mass spectrum is usually obtained by linearly increasing the DC and RF voltages, keeping their ratio and the oscillator frequency constant, allowing the successive emergence of ions of increasingly higher m/z.

Advantages of this design include the ease with which electric fields can be controlled, as opposed to magnetic fields, and the linear mass scale. The m/z range of commercial instruments is up to 4,000 with unit resolution throughout the range, although newer instruments can operate with peak widths of 0.1 m/z (FWHM). The small size, fast scan speed, relative mechanical simplicity of the device (although the ion motion itself is complex) and low construction costs are also attractive features of these instruments.

Another important use of these devices emerged with the realization that with the DC voltage set to zero and the RF maintained, the ions remained focused along the *z*-axis with relatively no mass selectivity. When operated in this RF-only mode (wide band pass) the assembly is used as an ion guide and as a gas phase collision cell in tandem instruments.

17. QUADRUPOLE ION TRAPS

QIT mass spectrometers first trap ions and in so doing no mass spectrum is recorded. The spectrum is only recorded when the ions of different m/z are

selectively expelled from the trap onto a detector. Thus, the operation is not continuous but involves a series of discrete steps in chronological order which include filling the trap with ions, removing unwanted ions that are outside the m/z range of interest, and then sequentially expelling the trapped ions and recording their m/z values and intensities. These instruments are 3D counterparts of the linear quadrupole mass filters described above. Wolfgang Paul and Helmut Steinwedel first described ion motion in these devices, but the demonstration of their potential practical utility came from the work of a number of individuals as detailed by March, Todd and Hughes, and from the work of George Stafford and colleagues at Finnigan Corporation [26–32].

The device consists of an evacuated cavity created by three hyperbolic surfaces (electrodes). These are a doughnut-shaped ring electrode and two end-capped electrodes (Figure 17). The layout resembles a 2D slice through a linear quadrupole mass filter. The instrument is operated by the application of DC and RF voltages to the ring and end-capped electrodes. Prior to 1984, the trap was operated in the mass-selective stability mode in which ions with a stable trajectory were stored by application of RF and DC voltages to the electrodes, and then ejected from the ion trap via a pulse of DC to an endcap electrode, to impinge upon an external detector, usually an electron multiplier. To obtain a mass spectrum, the RF and DC were scanned slowly at a constant ratio while the above scan function was repeated.

With only this mode of operation, the relative complexity of the scan function and the lack of any apparent advantage over linear quadupoles available at the time, hindered their development as analytical instruments. However, three important developments in the 1980s led to vast improvements in their operation. The mass-selective instability mode of operation, developed by Stafford et al., takes advantage of the low-mass cut-off inherent with all instruments of this design [32]. The low-mass cut-off refers to the m/z value below which ions have unstable trajectories and are lost from the trap. As a general rule of thumb, on commercial instruments the low-mass cut-off approximates to about one third of the m/z of the parent ion in the MS/MS mode. In the mass-selective instability

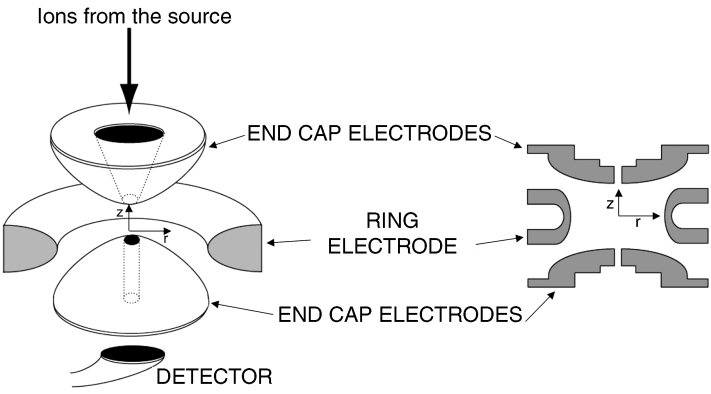

Figure 17 Schematic representation of a 3D quadrupole ion trap.

mode of operation, the trap is filled with ions in the RF-only mode with the voltage applied to the ring electrode and the end-capped electrode grounded. Under these conditions, the ions with m/z values above the low-mass cut-off have a stable trajectory within the trap. Then the RF on the ring electrode is increased (the end-capped electrodes remain grounded), and ions of increasing m/z are moved toward the point at which their trajectories become unstable. Upon reaching this point they are expelled from the trap in the z-direction and impinge upon the detector positioned outside the end cap electrode. In this way a complete mass range can be scanned with a single sweep of the RF, and if the RF is ramped linearly, the mass range is scanned linearly.

The next important development was the use of the bath gas. These instruments are almost always operated now in the presence of helium bath gas at relatively high pressure (approximately 1 mTorr). Without the bath gas the ions are distributed throughout the volume of the trap. In the presence of the bath gas the ions experience many non-fragmenting collisions with the helium, and in so doing loose kinetic energy. These collisions effectively dampen the oscillations of the ions and result in their confinement closer to the center of the trap. This results in a significant improvement in mass resolution and improved trapping of the ions introduced into the trap (sensitivity). The final important development came from appreciation of the significance of space-charge effects. With too many ions in the trap, space-charge influences of one ion upon the motion of another become significant. These effects must be minimal for good scan-to-scan reproducibility and accuracy of m/z assignment. The current instruments are able to adjust the filling time so that the trap contains an optimal population of ions to yield maximum sensitivity without significant space-charging.

Recent instrument designs include additional sophistication to the scan functions that result in significant improvements in resolution. For example, during the mass-selective instability scan of the RF, the addition of a resonant excitation voltage across the endcap electrodes at voltages sufficiently high to result in ion ejection significantly increases the mass resolution. Referred to as axial modulation, some designs apply the axial modulation frequency close to the low-mass cut-off region. By varying the applied frequency, the mass range of the ion trap can be increased and in addition high resolution across narrow m/z ranges scan can be achieved. Application of resonant excitation voltages at lower voltages causes kinetic excitation of mass-isolated ions, resulting in collision-induced dissociation (CID) to form product ions. This is the method by which fragmentation is induced in these instruments (see below).

QITs are relatively inexpensive devices that require low mechanical tolerances, operate at relatively high pressures (10^{-4}–10^{-3} Torr) and can trap mass-selected ions for seconds to minutes. Their low cost, small size, fast scanning capability and multiple operational modes has led to their widespread use. Note that in the linear quadrupole mass filter described above, ions with unstable trajectories are lost (i.e. not detected), whereas in the QIT ions need to acquire unstable motion before they escape the trap and be detected.

18. LINEAR ION TRAPS

Yet another type of quadrupole trapping device is now available [33]. The linear quadrupole design described above can be adapted as an ion trap by including two end electrodes (Figure 18). Ions injected into the device along the *z*-axis can be trapped radially by operating the quadrupole in the RF-only mode with helium (~3 mTorr) present as a kinetic energy damping gas. To prevent ions from escaping axially, a DC potential is applied to the end electrodes. Thus ions injected into the device will become trapped. This design is essentially a 2D ion trap in contrast to the 3D QIT described above. At any point ions can be expelled axially (along the *z*-axis), by removal of the DC potential on the end electrode, or radially, by ramping the RF voltages to increase the magnitude of the *x*–*y*

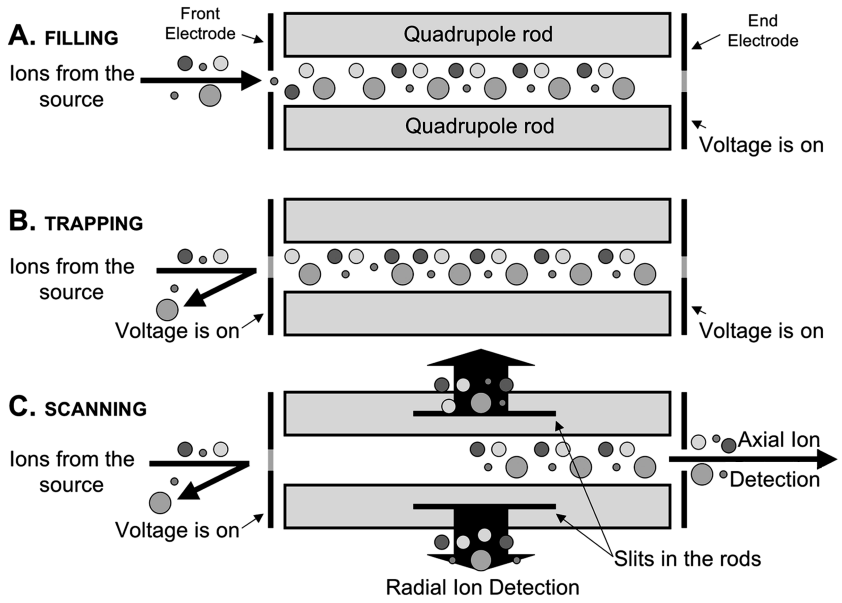

Figure 18 Schematic representation of the design and operation of a linear quadrupole ion trap. The device consists of set of quadrupole rods identical to those used in triple (or single) quadrupole mass spectrometers. At either end of the rods an electrode is placed. When the electrodes are energized the passage of ions is prevented. The electrodes can be in the form of a lens as shown, or a set of stubby quadrupole rods. (A) In the filling mode, the end electrode is energized, preventing ions from escaping out the back end of the trap. (B) Once the trap is full, the front electrode is also energized, thus preventing more ions from entering the trap and preventing the trapped ions from escaping. The trapped ions now oscillate along the length of the trap. (C) Two methods can be employed to record a mass spectrum. In axial ejection/detection the end electrode is de-energized, and a resonance voltage is applied to the rods to excite the ions, in a mass dependent fashion, out the back of the trap. In radial ejection/detection, the electrodes remain energized, and a resonance voltage is applied to force the ions out of the trap through slits cut into two of the rods. Radial detection requires the synchronized operation of two detectors, one positioned over each slit in the rods.

oscillations such that the ions exit in the x–y plane. This is equivalent to the mass-selective instability mode described for the QIT. Two designs are available commercially today: one with linear ejection of the ions, which requires a detector positioned in the normal position along the z-axis at the end of the device; and the other, which is less intuitive, by radial ejection of the ions. For radial ejection, two opposing electrodes (of the four) have slots cut in them behind which are situated dual detectors (electron multipliers), the operation of which must be synchronized. As with the 3D ion trap, in conjunction with the RF ramp, a resonant excitation voltage can be applied across the electrodes to increase the efficiency of ejection (sensitivity) and mass resolution. Advantages of this design over the QIT include enhanced trapping efficiency of injected ions, and the ability to trap significantly more ions prior to onset of significant space-charging. Both features result in the LIT having greater sensitivity over the QIT. LITs can be used as standalone mass analyzers, or more commonly in combination with other mass analyzers in tandem configurations. The tandem configuration takes advantage of the strong focusing of the ions along the z-axis.

19. ION CYCLOTRON CELLS AND FOURIER TRANSFORM MASS SPECTROMETRY

The principle of operation of ICR cells and FTMS is based on the fact that ions rotate in a plane perpendicular to a superimposed magnetic field in a direction defined by the so-called right-hand rule at a frequency dependant on their m/z. The rotating ions can be detected based on an image current that is induced in detector plates positioned outside of the cyclotron cell. The measured frequencies of the image current can be converted into m/z values with the cyclotron equation:

$$\omega = qB/m$$

where ω is the cyclotron frequency, q the charge on the ion, B the magnetic field strength and m mass of the ion (Figure 19).

Thus light ions have a high cyclotron frequency, and more massive ions have a lower frequency. Importantly, the cyclotron frequency does not depend upon the entering velocity or energy of the ion, partly explaining why the technique is able to produce such extraordinary high resolution.

The ions are trapped inside a cell that is positioned inside a unidirectional, constant and homogeneous magnetic field. The cell can be cubic, rectangular or, more commonly today, cylindrical. Under these conditions the ions are first stored in the cell where they undergo continuous rotation or cyclotronic motion at a very small radius (Figure 19). The ions are then excited to a larger radius of rotation by a pulse of radio-frequency energy. Ions with the same m/z are excited to a coherent cyclotronic motion. The characteristics of the cyclotronic motion are recorded as the frequency of the image current induced in detector plates that form the sides of the cell. The image current frequency is a composite sine wave consisting of the sum of the image currents formed by each packet of ions with

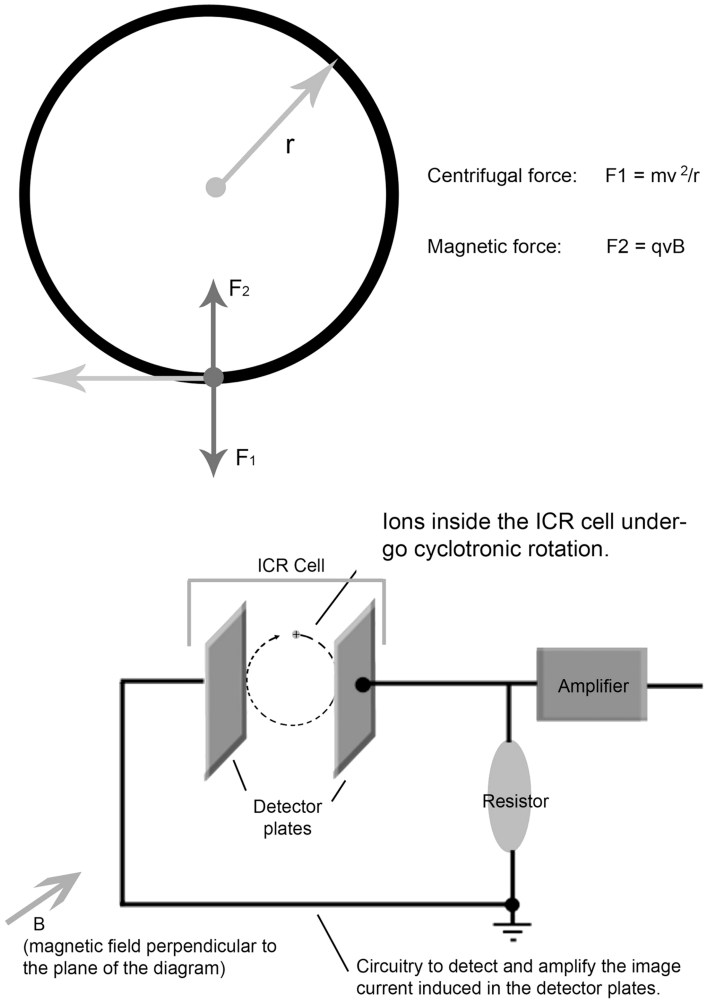

Figure 19 Principles of the Ion Cyclotron Resonance Cell. Top: Cyclotron motion results from a balance between the centrifugal force and the magnetic force. Bottom: Ions in a homogeneous magnetic field (B) move in circular orbits and in so doing induce image currents in the externally positioned detector plates. Adapted from ref. [34].

the same m/z. FT analysis is used to transpose the sampled image current measurements (referred to as the transient) from the time domain into the frequency domain. This has the effect of deconvolving the complex image current waveform into the individual contributions from the frequencies of each of the separate ion packets. The frequency domain data is easily translated into a mass spectrum by a simple calibration function. Cyclotron frequencies are measured with high precision, and the magnetic field is constant; these factors contribute to the production of spectra with unprecedented accuracy of m/z assignment and resolution.

In practice the physics works superbly provided the transients are not disturbed by collisions of the ions with gas molecules, or by interactions between the rotating ions (space-charge effects). For the production of accurate high-quality spectra the transients need to be stable for an adequate duration ($\sim$1 s for 100,000 resolving power at m/z 400 with a 7-T magnet), and space-charge influences of one ion upon the rotation of another must be minimal. Hence the requirement that the ICR cell be held at less than 10^{-9} Torr to minimize the collisions between an ion and a gas molecule, and the limit on the number of ions that can be tolerated within the cell ($\sim 10^4$–10^6 ions in a cubic centimeter cell). In addition, FT analysis requires adequate computing speed. The basic principles of ion cyclotron motion were described in the 1930s by Lawrence who was awarded the 1939 Nobel Prize in physics for developing the high-energy physics cyclotron and discovering the transuranium elements. The first ICR cells for organic mass spectrometry were built by John Baldeschwieler and colleagues [35]. The technique was quickly recognized for producing spectra with unprecedented resolution and accuracy of m/z assignment, but it did not gain widespread use until several obstacles were overcome. These include the development of the FT procedure for the rapid conversion of the transients to mass spectra, the availability of affordable computers with adequate data storage capacity and computing speed, the development of robust pumping systems that can achieve and maintain the necessary vacuum, the development of methods for introducing ions into the ICR cell from external ion sources, and the development of methods for accurately controlling or estimating the number of ions introduced into the ICR cell [36–37]. Commercial instruments today use wide-bore superconducting magnets with field strengths in the range 7–15 T. The tandem combination of a LIT with an ICR cell is a successful configuration with which the introduction of ions from an external ion source can be accurately controlled. This configuration is finding widespread application, particularly within the proteomics field.

20. THE ORBITRAP

The orbitrap mass analyzer is the first fundamentally new mass analyzer introduced commercially in over 20 years. The device is an ion trap but there are no RF or magnetic fields. Moving ions are trapped as they rotate around an electrode, with electrostatic attraction toward the electrode balanced by the centrifugal force arising from the rotation. This trapping principal was first implemented in the Kingdon trap [38], then modified by Knight [39] and finally developed by Makarov [40] as the basis for the orbitrap analyzer. In it the ions are trapped in a high electrostatic field and allowed to orbit a spindle-shaped central electrode within a barrel-shaped outer electrode (Figure 20). The axial frequency of harmonic oscillations is inversely proportional to the square root of the m/z, and the resulting image current is recorded in the time domain similarly to image currents in FT-ICR instruments. Such a design represents an alternative to the magnet-based ion cyclotron motion used for mass analysis in an ICR cell.

Note that, unlike the FT-ICR where the motion along the z-axis is ignored and it is motion in the x–y plane that is measured, in the orbitrap, it is the z-motion that is measured and the x–y motion that is ignored.

The development of the technology into a useful mass spectrometer required implementation of a several technological advances [41]. One fundamental problem was that of introducing ions into the orbitrap from an externally positioned ion source. Ions coming from the outside into a static electric field will normally continue unabated through the field and emerge on the other side, much like the passage of comets across the solar system. By lowering the voltage on the central electrode during the ion introduction step, it is possible to allow the ions to remain in the electrostatic field and assume a cyclic rotation around the central electrode. This in effect traps the ions, and is referred to as electrodynamic squeezing.

The next advance involved developing a technology for introducing ultra-short packets of ions ($<1\,\mu s$ duration) from the external ion source. The introduction of ultra-short packets of ions is necessary if the resulting spectra are to have resolutions approaching those theoretically possible. A solution to this problem emerged with the development of the so-called "C" trap, an RF-only (i.e. non-mass selective) curved quadrupole in which ions are stored and their vibrations dampened by non-fragmenting collisions with a bath gas. The exit from the C-trap is positioned opposite the entrance, but displaced from the equatorial circumference of the orbitrap (Figure 20). Thus short packets of ions are injected from the C-trap by application of a DC voltage and converge on the orbitrap entrance. Ions entering the orbitrap are trapped by the electrodynamic squeezing phenomena, and assume a cyclic rotation around the central electrode. The ions move to and fro, along the z-axis of the trap as dictated by the spindle-shaped curvature of the electrode. Ions of the same m/z develop coherent motion and gather as a ring-shaped cloud, much like the rings of Saturn. The frequency of transverse movement of these clouds of ions in the z-axis is recorded on split outer electrodes, and the time domain signal is converted into an m/z signal by fast Fourier transformation.

The current status of this instrument is that resolutions between 20,000 and 160,000 across the 100–10,000 m/z range ($M/\Delta M$) can be routinely achieved, and as already stated, very recent results with internal lock mass calibration show that sub ppm accuracy is possible making this a high-performance instrument suitable for many applications (Joshua Coon and refs. [42,43]).

21. DETECTORS

The final component of the mass spectrometer depicted in Figure 1 is the detector. Most mass analyzers produce a beam of ions that can be detected as an electrical current when the beam impinges upon a responsive surface. For example, currents of the order of picoamps are typically produced by ESI sources after amplification by an electron multiplier. Some detectors measure ion current, and some detectors count ions. The types of devices that are used to detect the ion

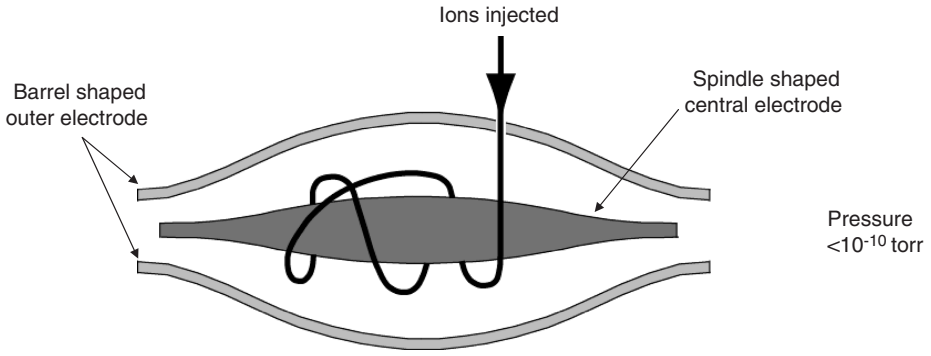

Figure 20 Schematic representation of an orbitrap. The approximate ion path is shown. Ions are injected into the device in short packets ($<1\mu$s duration) from a curved linear ion trap (not pictured) positioned orthogonally to the orbitrap. Injected ions of the same *m/z* assume a coherent rotation around the spindle-shaped central electrode, and the frequency of their transverse oscillations is recorded. Adapted from a Thermo Scientific instrument design.

beam include electron multipliers, photomultipliers and multichannel plates. Off-axis positioning of the device is common to avoid recording the impact from neutral species that would otherwise cause a high background signal. High-energy conversion dynodes are also used to magnify the signal from an incoming ion (see below). Focused ion beams are detected by point detectors that include electron- and photomultipliers, and dispersed beams are detected by array detectors which include multichannel plates.

ICR cells and the orbitrap are unusual in that they use a different, non-destructive method for detecting the ion beam. Both these instruments are ion traps and contain a population of ions that coherently move within the confines of the trap in a manner dependent on their m/z. The rotating ions generate an image current on appropriately positioned plates at the side of the trap, and the systems work by translating the time-domain image current data into the frequency domain, and then subsequently converting those frequencies into a mass spectrum.

22. ELECTRON MULTIPLIERS

These are common detectors on quadrupole, QIT and LIT instruments. When energetic ions collide with a suitable solid surface (one that requires a relatively small amount of energy to remove an electron from the surface, referred to as a surface with a low workfunction), electrons are liberated. The conversion of ions to electrons and subsequent electron amplification can be achieved using discrete collisions on separate electrodes (dynodes), the potentials of which are arranged so that electrons are accelerated from one stage to the next producing a cascading effect, for example, the so-called venetian blind electron multipliers.

Alternatively, one can apply a potential across a semi-conductor material so that the electrons produced in one collision event are accelerated into the device to undergo further electron-surface collisions. Typically 10–20 stages of electron amplification are used. A single electron gives 10^6 electrons in just 12 stages of gain, when the average gain factor on each collision is just 3.3, a typical number.

23. CONVERSION DYNODES OR HIGH-ENERGY DYNODES

The velocity of the incoming ions determines the probability and number of electrons released from the low workfunction surface of the electron multiplier. As a result, high mass ions, which are relatively slow moving, even at the customary energies of a few keV, often need to be converted into smaller, more energetic ions. This initial ion-to-ion conversion is achieved by impact of the primary ions onto a suitable dynode conversion surface. Ions and electrons resulting from impact with the dynode are accelerated into the throat of an appropriately positioned electron multiplier for further amplification of the signal. Negative ions are detected with electron multiplier operating at the same potentials as for positive ion detection, but with the conversion dynode at the opposite polarity.

24. QUANTIFICATION

Precise quantification is only achieved by using an internal standard (IS). The rationale for the use of an internal standard (IS) is to compensate for errors that are otherwise difficult to control. Such errors include variations in the yield of a purification process and chemical modification, for example disulfide reduction, thiol alkylation, ezymatic or chemical digestion, etc., and losses due to adsorption on glassware and chromatographic surfaces. The best internal standard is one that has physical and chemical properties that are as similar as possible to those of the analyte in question. Chemical analogues are often used as ISs, but molecules labeled with stable isotopes of low natural abundance (e.g. ^{2}H, ^{13}C and ^{14}N and ^{18}O) are the preferred choice. In the case of stable isotope-labeled ISs there is virtually no distinction made in the analytical experimental work-up between the naturally occurring molecules and the IS, either by adsorption or during extraction and derivatization. Furthermore, because of the usual co-elution of the IS and analyte, they are subjected to the same mass spectrometric conditions. Mass spectrometry has the unique ability to distinguish between such closely related molecules and provides a ratio of their signal intensities. Provided an absolute standard is available, this ratio can be converted to moles of analyte. Without an absolute standard, one is left with relative quantification. The recently developed iTRAQ™ and related methods for peptide (protein) quantification with MS rely on measurement of relative analyte amounts in different samples.

The example selected to demonstrate the principles of quantification by mass spectrometry uses GC/MS, but the same principles apply regardless of the method by which samples are introduced into the mass spectrometer (Figure 21). In this example the task was to measure the absolute concentrations of a serotonin metabolite (5-hyroxyindoleacetic acid, 5HIAA) in human cerebrospinal fluid (CSF), which surrounds the brain and spinal cord. Five standard samples were prepared in an isotonic salt solution (artificial CSF) with known amounts of

Sample	Human CSF (ml)	Added unlabelled analyte ng	Added labelled internal standard ng	Analyte peak height	Internal standard peak height	Analyte/ internal standard ratio	Analyte in human CSF (ng)
Standard 1	0	0.00	15.0	12	2077	0.01	
Standard 2	0	2.80	15.0	1224	4835	0.25	
Standard 3	0	6.99	15.0	2163	3578	0.60	
Standard 4	0	13.98	15.0	4916	4295	1.14	
Standard 5	0	21.96	15.0	9775	4522	2.16	
Unknown 1A	1		15.0	1001	984	1.02	11.1
Unknown 1B	1		15.0	1781	1768	1.01	11.0
Unknown 2A	1		15.0	2833	2816	1.01	10.9
Unknown 2B	1		15.0	2031	1874	1.08	11.8
Unknown 3A	1		15.0	623	504	1.24	13.4
Unknown 3B	1		15.0	1341	1157	1.16	12.5

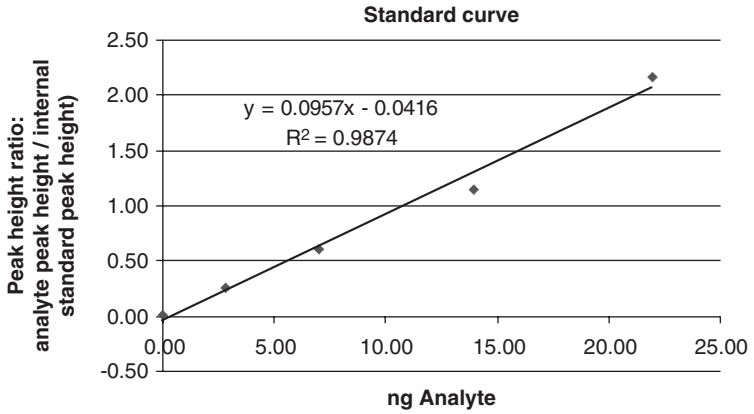

Figure 21 Quantitation using selected ion monitoring with a deuterated internal standard. Data set from an experiment in which the concentration of 5-hydroxyindole acetic acid (5HIAA, analyte) was measured in human lumbar cerebrospinal fluid (CSF) using $^{2}H_{2}$-5HIAA as the internal standard. The experimental setup is as described in the text. The amount of analyte in each human CSF sample was calculated by interpolation from the standard curve.

authentic 5HIAA (0–22 ng), and three samples of human CSF were prepared in duplicate (A and B series). The same amount of IS ($^2H_3$-5HIAA, 15 ng) was added to the standards and the human CSF samples. All samples were then processed in the same manner by extraction with an organic solvent, concentration under a stream of nitrogen gas, chemical derivatization and analysis by GC/MS [44]. The SIM traces for the signals corresponding to the molecular ions of 5HIAA (m/z 622) and IS (m/z 625) were recorded, and the absolute peak heights (arbitrary units) for these two virtually co-eluting signals are shown in Figure 21, along with the ratio of their peak heights (R, 5HIAA/$^2H_3$-5HIAA peak height). Calibration curves prepared from the data for the standard samples show that the absolute peak height for 5HIAA, and the *R*-values, are linear when plotted against the amount of added 5HIAA. However, the absolute peak heights for 5HIAA in the duplicate samples from human CSF vary widely, reflecting experimental variations that result from the extraction, derivatization and injection procedures. However, the *R*-values for the same samples agree within the errors expected for this type of work. Thus the amount of $^2H_3$-5HIAA in each human CSF sample can be accurately computed by interpolation from the standard curve using the *R*-values. This example reveals the value of using an IS to correct for errors that unavoidably occur during sample preparation and analysis.

25. STRUCTURAL ELUCIDATION BY MASS SPECTROMETRY

Desorption and spray ionization methods tend to produce abundant molecular ions with little or no fragmentation. This is ideal for determination of molecular weights, but provides no information on structural details. One approach to this problem would be to fragment or dissociate the ion and measure the m/z values of the resulting charged fragments. For proteins and peptides, dissociation can be induced by collision with a gas molecule (CID also known as collisionally activated dissociation (CAD)), or capture of an electron (electron capture dissociation, ECD), or an electron transfer dissociation (ETD). Provided the dissociation of the parent ion is not a random process and that certain bonds break easier than others, such an experiment should yield useful structural information. Dissociation induced by such processes is not random but highly reproducible, and the rules governing fragmentation of many classes of gas phase ions, including those from peptides, are now known. The spectra of fragment ions generated in this way can often be interpreted to yield a sequence, or more commonly a partial sequence. These experiments are referred to as tandem mass spectrometry (MS/MS), and an arrangement of analyzers within an instrument in which such an experiment could be performed is represented schematically in Figure 23. There has been a long history to the development of different methods to induce fragmentation of gas phase ions, including intense electromagnetic radiation (laser-induced fragmentation), collisions with an inert surface (surface-induced dissociation), photodissociation and infrared

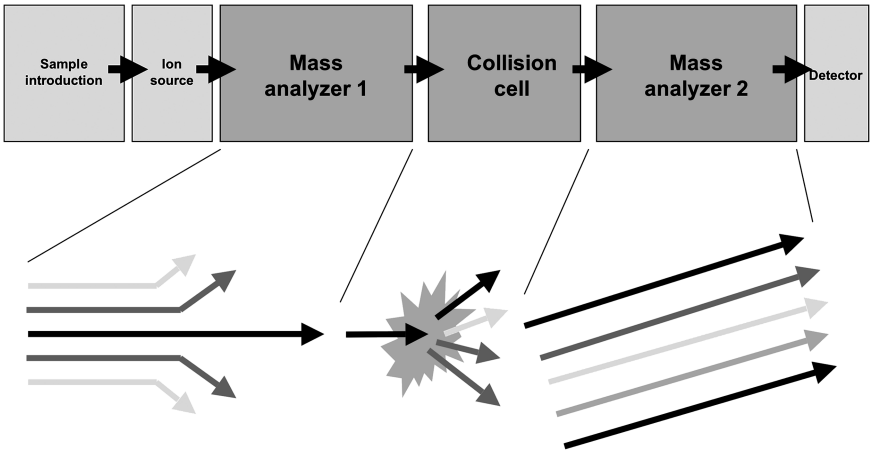

Figure 22 Structural elucidation by MS/MS.

multiphoton dissociation (IRMPD). Today for protein chemistry the most important methods are CID, usually with argon or nitrogen, ECD and ETD.

MS/MS experiments can be carried out by positioning two mass spectrometers in series (referred to as MS1 and MS2), separated by a collision cell in which dissociation is induced (Figure 22). The operation of the two analyzers requires synchronization of their scan modes. A successful tandem design can be assembled with identical analyzers for MS1 and MS2 (e.g. two double focusing magnetic sector instruments, or more commonly, two quadrupole, or two TOF analyzers), or with dissimilar analyzers for MS1 and MS2 (e.g. hybrid quadrupole/TOF instruments). However, experiments such as these can also be conveniently carried out using a single trapping mass spectrometer (QITs and LITs): by isolating a specific parent ion, allowing the parent to fragment, and then measuring the m/z values of the resulting charged fragments. In this case, the experiment is performed with a single analyzer with obvious cost advantages.

26. GAS PHASE ION STABILITIES AND ENERGETICS OF THE COLLISIONALLY-ACTIVATED DISSOCIATION PROCESS

In the gas phase a distinction is drawn between ions in three different stability regimes. These are unstable ions of high internal energy with dissociation rates $>10^6\,s^{-1}$ that are not observed in mass spectra, stable ions with low internal energy and dissociation rates $<10^5\,s^{-1}$ that constitute the bulk of the ion current observed in mass spectra and selected for fragmentation in MS/MS experiments, and finally metastable ions with intermediate internal energy and dissociation rates between 10^6 and $10^5\,s^{-1}$ that fragment between the ion source and detector. Metastable ions are occasionally observed in mass spectra as broad poorly resolved peaks.

Depending on the energy absorbed by the parent ion, there are two possible fragmentation pathways dictated by the energy regime. Most MS/MS instruments work in the low-energy regime, while high-energy ion fragmentation typically occurs in tandem TOF and tandem magnetic sector instruments. Ions undergoing low-energy fragmentation have an average internal energy of 10–100 eV, whereas ions undergoing high-energy fragmentation have an average internal energy of a few keV [45]. These two modes also differ by the fact that the low-energy mode involves multiple collisions, whereas high-energy fragmentation often involves a single collision event. In general, fragmentation of a parent ion can occur when the transmitted collision energy is sufficiently high that the ion is excited beyond the dissociation threshold. Regardless of the mass spectrometer used, the selection window for the parent ion is an important parameter. A narrow window imparts greater selectivity in the process by restricting the experiment to a homogeneous population of parent ions, but a wide window will increase signal strength of the product ions, and hence sensitivity. Quadrupole and QITs can be tuned for a wide range of parent ion acceptance windows from wide ($> \pm 1.0$ Da) to unit (± 1.0 Da) to narrow ($< \pm 1.0$ Da). There is less flexibility in parent ion acceptance window selection with TOF analyzers, and they are generally operated with a-3–10-Da wide selection gate.

27. COLLISION-INDUCED DISSOCIATION

CID describes an ion species interaction wherein the projectile ion is dissociated as a result of interaction with a target neutral species. This is brought about by conversion of part of the translation energy of the ion to internal energy in the ion during collision. CID can occur in the ion source-mass analyzer interface, where ions in the gas phase emerging from the source encounter residual gaseous molecules from the atmosphere and drying gas. There is no parent ion selection with these events, so interpretation of the resulting fragment ion spectrum can be difficult. In contrast, CID can also occur in the collision cell that is positioned between the two analyzers of the tandem mass spectrometer. In this case there is opportunity for parent ion selection, and interpretation of the resulting fragment ion spectrum is not confounded with uncertainty about the m/z of the parent ion. The efficiency of CID may be increased by using a more massive gas, such as argon or xenon. With different instruments, CID can be carried out with high (keV) or low (10–100 eV) collision energies with some differences being noted in the types and relative abundances of the product ions. However, low-energy CID MS/MS experiments are, by far, the most common method used to dissociate peptide ions.

Although gas phase dissociation of peptides has been investigated for many years, and the general rules governing the process are known, it remains as an important field of ongoing research because *de novo* peptide sequencing is still a challenge. This is of particular importance because of the increasing numbers of MS/MS spectra generated through automated MS methodologies and used for

protein identification through database searches. The general model used to explain peptide fragmentation in the gas phase is called the "mobile proton model" [46]. The idea behind this is that bond cleavages are charge directed. During ionization, protonation occurs on basic sites and the population of different protonated forms of a peptide or a protein depends on both the internal energy of the ions, as well as the gas phase basicities of protonation sites. There is a correlation between gas phase basicities of protonation sites and the energy required to induce fragmentation. The presence of a charge at a specific site may promote the fragmentation of adjacent bonds. For example, protonation at the peptide backbone initiates charge directed cleavages at the peptide skeleton leading primarily to cleavage of the amide bond and production of so-called *b*- and *y*-type ions (Figure 23). Peptides carrying a basic amino acid in the C-terminus (e.g. peptides produced by trypsin digestion) tend to show more intense and higher m/z *y*-ions in the spectra, attributed to the stability of these ions. The corresponding *b*-ions are thought to fragment further because the charge site is mobile, and thus they appear as less intense signals in the lower m/z region of the spectra. Although peptide CID spectra are generally dominated by *b*- and *y*-type ions, there are other ions formed, and the spectrum of fragment ions produced can be complex. For example, *b*-ion isomerization leads to proton

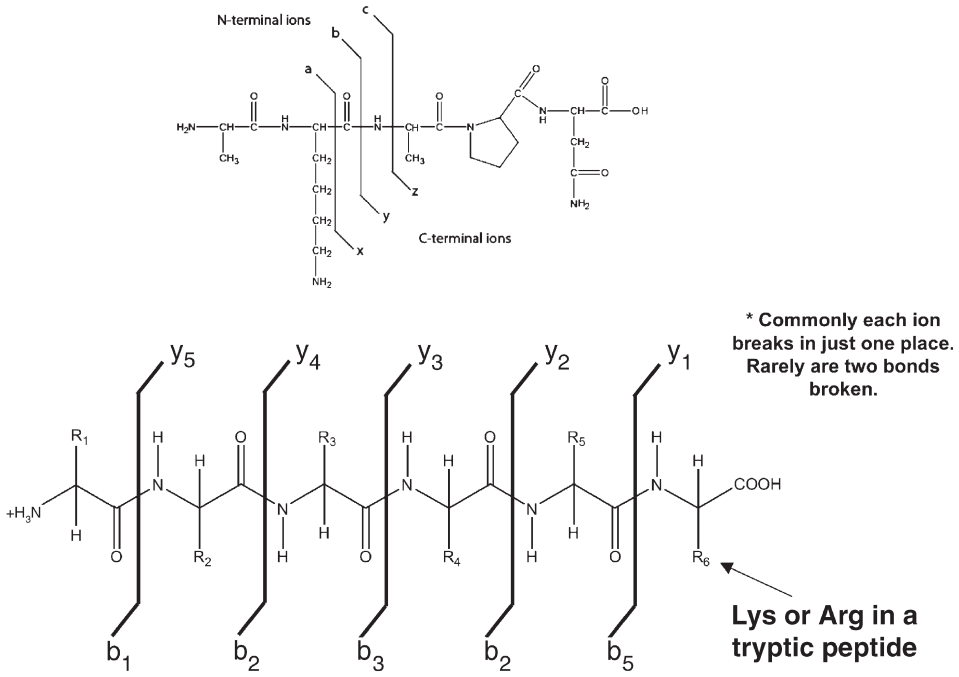

Figure 23 Peptide fragmentation nomenclature in which *y*-type ions contain the C-terminus, and *b*-type ions contain the N-terminus of the peptide.

scrambling that is the random movement of protons within an ion, while charge remote fragmentation results in the neutral loss of water and ammonia [47–49]. In addition, production of internal fragments resulting from multiple collisions that occur with low-energy MS/MS instruments, is another frequently observed feature of peptide CID spectra [48,50]. The difficulties in *de novo* peptide sequencing with CID arise primarily from incomplete *b*- and *y*-ladders in the spectra, but insufficient or overabundant fragmentation, or unusual and unexpected fragmentation processes also complicate interpretation of the spectra. Recently, a comprehensive study of synthetic peptides sharing common features showed that half of the compounds displayed low-energy fragmentation patterns that were in agreement with the mobile proton model [47]. The remaining half of the peptides underwent alternative dissociation pathways with complex rearrangements. These unusual fragmentation processes include charge remote fragmentation, intra-molecular interactions, gas phase rearrangements and *b*-ion scrambling.

Apart from the difficulties for *de novo* peptide sequencing mentioned above, other important deficiencies in CID spectra also include ineffectiveness for probing site-specific chemical modifications, especially labile post-translational modifications such as phosphorylation and some glycosylations. To overcome these limitations other fragmentation modes have been investigated. The most useful to date, ECD and ETD, appear to offer needed complimentarity to the CID process. Both ECD and ETD use low-energy electrons to promote fragmentation of the peptide backbone, and differ only in the way that low-energy electrons are transferred to gas phase peptide and protein ions.

28. ELECTRON CAPTURE DISSOCIATION

ECD was first introduced by McLafferty and colleagues in 1998, and since then has been demonstrated to be efficient causing its use to become increasingly wide spread (see Zubarev, this volume) [51–54]. In an ECD experiment, multiply charged ions are trapped in an ICR cell and allowed to react with near-thermal energy electrons ($\leqslant 0.2$ eV) produced within the cell with an electron gun. Capture of such an electron by a protonated peptide is exothermic by ~ 6 eV, and yields peptide backbone fragmentation in a non-ergodic manner. Two phenomenon are then observed; partial neutralization of the parent ion leading to the charge state reduction, and extensive backbone cleavage yielding predominantly *c* and $z^{\bullet}$ fragment ion series (Figure 24). This is in contrast to CID dissociation that, as already stated, produces predominantly *b*- and *y*-fragment ions. Whereas *b*- and *y*-fragment ions originate from the cleavage of the amide bond, *c* and $z^{\bullet}$ fragment ions result from the N-Cα amine backbone (Figure 23). Thus the ECD and CID processes produce complimentary fragmentation patterns. ECD does not exclusively produce *c* and $z^{\bullet}$ fragments as there is some production of *b*- and *y*-fragments with restricted fragmentation N-terminal to proline residues [55–58].

In the ICR cell, ECD works on a millisecond timescale with an efficient precursor to fragment ion conversion rate of about 30%. This reaction timescale is

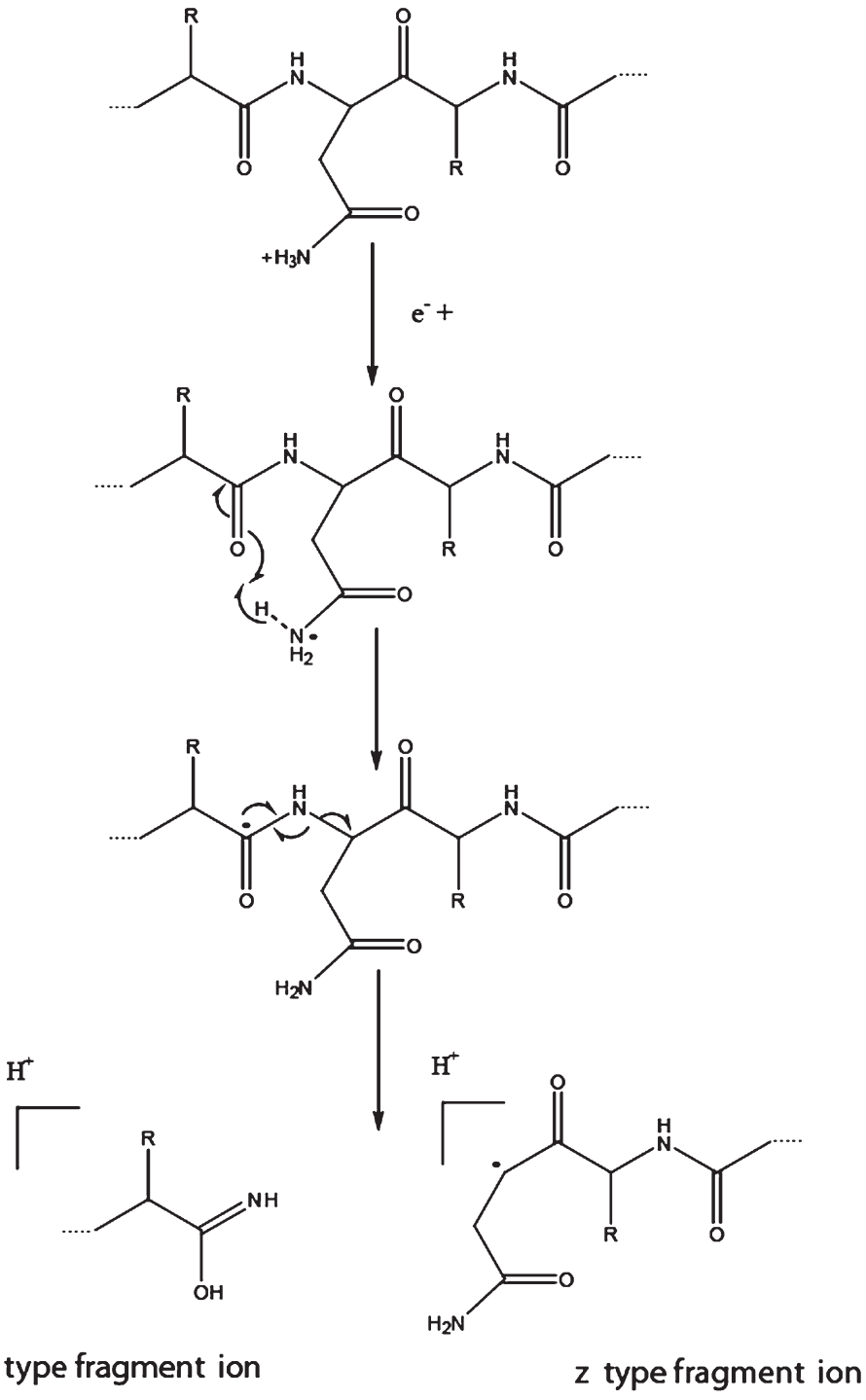

Figure 24 Scheme of the ECD process.

compatible with all forms of liquid chromatography in use today, providing ample time for the collection of many spectra during the elution of a single chromatographic peak. The process typically produces fragment ion spectra with near-uniform signal intensity of the fragment ions. This is in contrast to CID spectra in which the intensity of the fragment ions can vary dramatically. Importantly, because the peptide backbone cleavages occur in an independent manner, this process preserves labile chemical modifications that are often lost during CID. Ongoing investigations are focusing on the use of this technique for characterization of labile modifications such as phosphorylation, *O*-glycosylation, acylation, sulfation and nitration [7,51,59–61].

Another important impact of ECD in the biological mass spectrometry field is the development of ''top-down'' analyses of proteins. The ''top-down'' approach refers to the direct MS/MS fragmentation of intact proteins in the gas phase for their identification and characterization. Recently, ECD experiments were shown to preserve quaternary structures in the gas phase and could be used in the future to probe arrangements of protein complexes [62].

29. ELECTRON TRANSFER DISSOCIATION

The main drawback of ECD is that it can only be implemented on instruments in which near-thermal electrons have a sufficiently long residence time (milliseconds or longer) to allow reaction with gas phase analyte ions. Such electrons have long residence times in ICR cells, and the technique can only be used today on FTMS instruments. ETD was developed to implement the same reaction on other ion trap mass spectrometers [63,64]. In this process, low-energy electrons are transferred to multiply charged peptide ions using gas phase ion–ion chemistry. The kinetics of such chemistry have long been known, and electron-donating species, such as gas phase anthracene anions, are used to deliver the electrons to the isolated parent ions of interest. The gas phase electron-donor ions, generated outside the reaction chamber by a separate ionization process, most commonly electron capture chemical ionization of gas phase molecules, are injected into the reaction chamber to catalyze the ETD process. This method is analogous to ECD and produces *c* and $z^{\bullet}$ fragment ions with similar efficiency and relatively uniform intensity. ETD also preserves labile post-translational modifications. Benefits are the same as for ECD, and include the ability to analyze large and non-tryptic peptides with complete or nearly complete sequence coverage, including post-translationally modified residues [53,65]. The ability to perform this type of fragmentation on less expensive and widely used ion trap instruments is leading to the widespread use of this fragmentation method in protein mass spectrometry.

30. SCAN MODES IN TANDEM MASS SPECTROMETRY

The linear arrangement of two scanning mass spectrometers in series, shown simplistically in Figure 22, is a logical design that provides a unique analytical

platform with which multiple types of experiments can be performed. The product (fragment) ion scan has already been introduced: a parent ion is selected in MS1, fragmented in the collision cell, and the m/z of the resulting charged products (fragments) are recorded by scanning MS2 (Figures 25 and 26A). The reverse experiment can be performed in which MS1 is scanned and MS2 is set to transmit a single product (Figure 26B). This experiment, referred to as a "parent ion scan" yields the m/z of the parent ions that give rise to a common product. A third scan modality can be implemented in which both MS1 and MS2 are scanned with a set m/z offset (Figure 26C). This neutral loss scan will record the m/z of all parent ions that undergo the same m/z loss upon fragmentation. In the field with which this volume is concerned (protein mass spectrometry), product ion and neutral loss scans are the most important. Product ions scans yield fragmentation patterns that are used to sequence and identify peptides. Neutral loss scans are used to identify peptides that lose unique masses upon collisions,

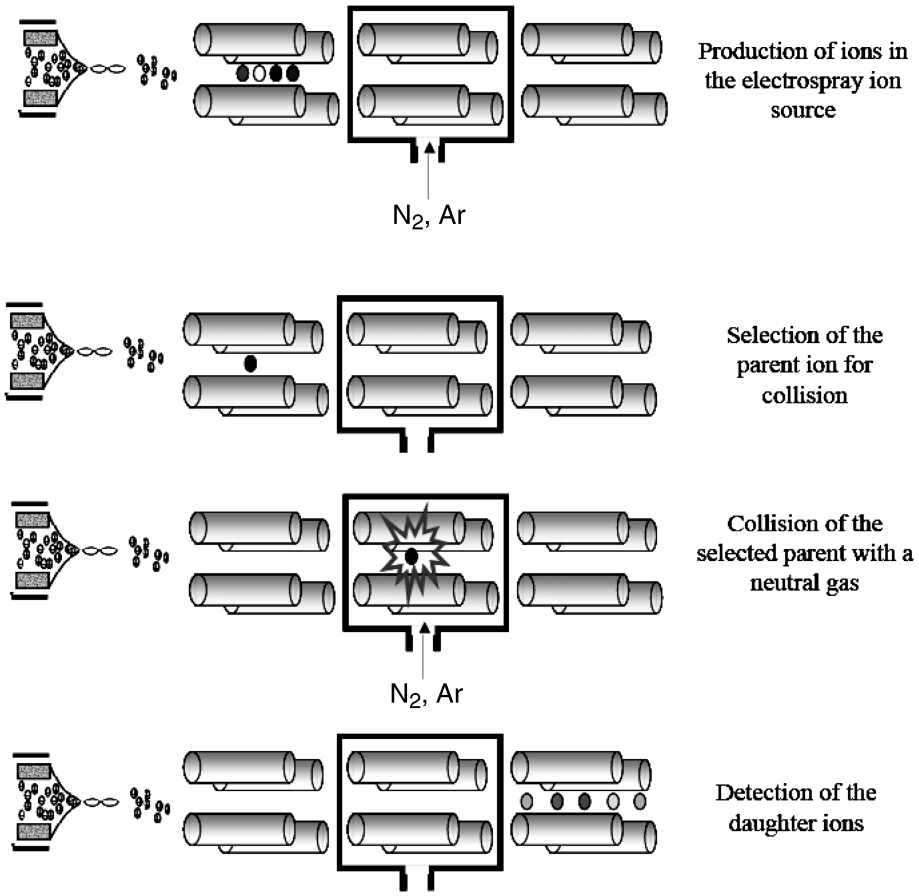

Figure 25 Scheme of events that take place during a fragment ion scan.

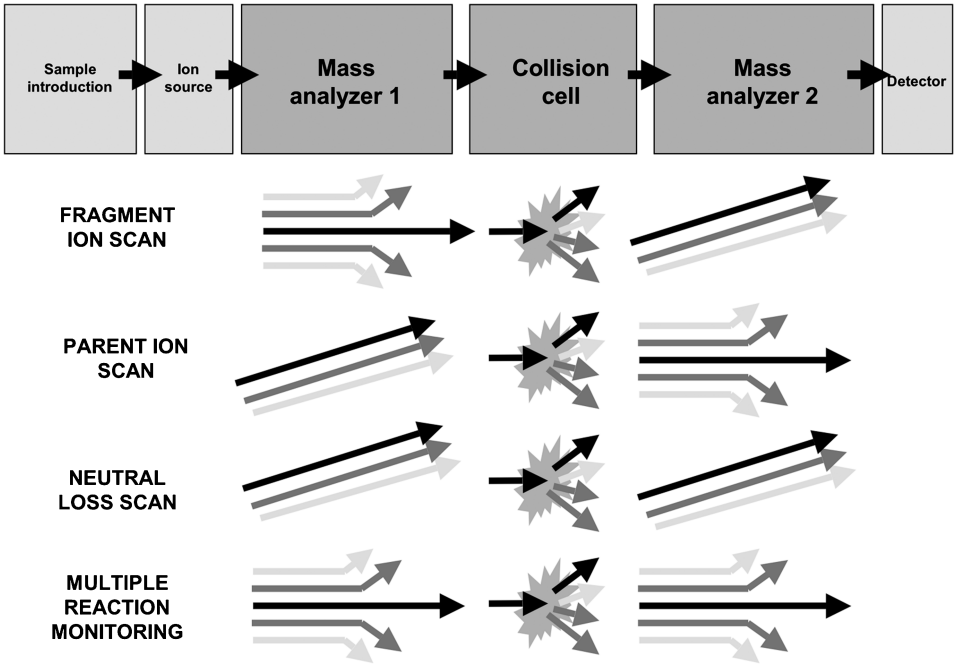

Figure 26 Triple quadrupole scan modes.

such as 97 Da from the loss of a molecule of phosphoric acid (H_2PO_4) as occurs readily during CID of phosphopeptides.

For quantitative experiments there is yet another scan mode that is used. If MS1 is set to transmit a single parent (P), and MS2 set to transit a single fragment (F), then the resulting trace will represent the intensity from the $P \rightarrow F$ transition (Figure 26D). This mode of data collection, referred to as "reaction monitoring", can only be employed when the parents and the products are known, and is usually done in combination with chromatography. With an appropriate IS the relative intensity of the transition for the analyte ($P_A \rightarrow F_A$) and reference compound ($P_{IS} \rightarrow F_{IS}$) is a quantitative ratio, and the amount of analyte in the sample can be accurately calculated from the ratio if the molar responses of the two compounds are known. Modern instruments are capable of monitoring many $P \rightarrow F$ transitions during the time taken for elution of a single chromatographic peak. Thus it is generally referred to as "multiple reaction monitoring" (MRM).

The four scan modalities (fragment ion scan, parent ion scan, neutral loss scan and MRM) described above and in Figure 26 can be performed in tandem mass spectrometers with a linear arrangement. However, certain combinations of instrument types for MS1 and MS2 are better for some of these experiments. By far the most successful and versatile combination of instruments is that of a dual quadrupole arrangement. In this design, the collision chamber is also a quadrupole, but operated in the RF-only mode to focus the incoming and out-going ion beams along the *z*-axis to reduce scatter resulting from collisions

and improve ion transmission efficiency. Thus these instruments are called triple quadrupoles, frequently abbreviated as triple quads, or QQQ or QqQs.

MS/MS can be achieved without two linked analyzers with a QIT instrument. The ions from the sample are injected into the trap and held there briefly. All unwanted ions are then ejected leaving the desired parent ion. This is done by operating with RF and DC potentials such that only ions of a single m/z have stable trajectories. The behavior of the chosen parent ion can then be observed in isolation. It is possible to supply a supplementary RF potential at an appropriate frequency to excite these ions. In the absence of the helium bath gas the ions would gain kinetic energy, develop an unstable trajectory and be lost from the trap. However, in the presence of the helium bath gas, collisions between the retained and excited parent ions and the bath gas occur, converting some of the kinetic energy of the ions into internal energy, hence exciting them internally and facilitating dissociation. A conventional scan then reveals the resulting product ions. This CID event is efficient if the excitation voltage is optimized. With QITs the processes of parent selection, fragmentation and fragment detection, are separated in time, not space, as in a QQQ instrument. However, the product ion spectra produced by both MS/MS methods (QIT and QQQ) are surprisingly similar.

Some, but not all of the scan modalities described above and in Figure 26 can be performed in QITs. Most notably, the parent scan modality is theoretically impossible because the parent ions are lost before the product ions are detected in the QIT. This shortcoming can be at least partially offset by the development of software for reconstruction of the data set after all parents have been individually fragmented, a feature that is possible to implement on a practical basis because of the exceptionally fast scanning ability of new QIT designs. The QIT design, however, offers an important advantage over the QQQ design for other applications. Multistage CID MS/MS experiments, referred to as MS^n, are possible on a QIT. In a linear format such experiments would require multiple mass analyzers. Although restricted to fragment ion scans, this technique is advantageous for the elucidation of structural details and fragmentation pathways that are beyond the reach of MS/MS experiments. For example, MS^n is finding important application in elucidating the fine structure of the glycosyl moieties attached to proteins.

31. CONCLUSIONS

The field of mass spectrometry has witnessed a phenomenal development over the past decade. This may be intimidating to the novice in the field. However, the principles upon which the technique is based do not change, and a sound grasp of these principles will place a new student in a position to understand and appreciate the potential that this technique offers. In this chapter we have attempted to lay the groundwork for understanding these principles in simple, non-technical terms. It is hoped that with this information at hand the subsequent chapters in this volume can be fully appreciated by all those wishing to learn more about this important and exciting field.

ACKNOWLEDGEMENTS

The authors wish to acknowledge the advice received from Franz Hillenkamp, John Fenn, Alexander Makarov and Robert McIver, who read and edited selected portions of this chapter, Hans Barnard for his excellent editorial advice and Jae Oh Yoon for help with some of the figures.

REFERENCES

1 P.S.H. Wong and R.G. Cooks, Ion trap mass spectrometry, *Curr. Sep.*, 16(3) (1997) 85–92.
2 M.A. Grayson (Ed.), *Meauring Mass: From Positive Rays to Proteins*. Chemical Heritage Press, Phildelphia, PA, 2002.
3 C. Brunnée, The ideal mass analyzer: Fact or fiction, *Int. J. Mass Spectrom. Ion Process.*, 76 (1987) 121–237.
4 D.F. Torgerson, R.P. Skowronski and R.D. Macfarlane, A new approach to the mass spectrometry of non-volatile compounds, *Biochem. Biophys. Res. Commun.*, 60 (1974) 616–624.
5 M. Barber, R.S. Bordoli, R.D. Sedgwick and A.N. Tyler, Fast atom bombardment of solids as an ion source in mass spectrometry, *Nature*, 293 (1981) 270–275.
6 K. Tanaka, H. Waki, Y. Ido, S. Akita, Y. Yoshida and T. Yoshida, *Rapid Commun. Mass Spectrom.*, 8(2) (1988) 151–153.
7 M. Karas and F. Hillencamp, Laser desorption ionization of proteins with molecular masses exceeding 10,000 daltons, *Anal. Chem.*, 60 (1988) 2299–2301.
8 J.B. Fenn, M. Mann, C.K. Meng, S.F. Wong and C.M. Whitehouse, Electrospray ionization for mass-spectrometry of large biomolecules, *Science*, 246(4926) (1989) 64–71.
9 A.L. Burlingame, M. Calvin, J. Han, W. Henderson, W. Reed and B.R. Simoneit, Lunar organic compounds: Search and characterization. *Earth, Moon, Planets*, 1(3) (1970) 396 (Proceedings of the Lunar Science Conference, Houston, Texas, USA, January 5–8, 1970).
10 M.S.B. Munson and F.H. Field, Chemical ionization mass spectrometry. I. General introduction, *J. Am. Chem. Soc.*, 88 (1966) 2621–2630.
11 J.M.L. Mee, J. Korth and B. Halpern, Rapid and quantitative blood analysis for free fatty acids by chemical ionization mass spectrometry, *Anal. Lett.*, 9(12) (1976) 1075–1083.
12 J.M.L. Mee, J. Korth, B. Halpern and L.B. James, Rapid and quantitative blood amino acid analysis by chemical ionization mass spectrometry, *Biomed. Mass Spectrom.*, 4(3) (1977) 178–181.
13 C.M. Whitehouse, R.N. Dreyer, M. Yamashita and J.B. Fenn, Electrospray interface for liquid chromatographs and mass spectrometers, *Anal. Chem.*, 57(3) (1985) 675–679.
14 M.P. Washburn, D. Wolters and J.R. Yates, Large-scale analysis of the yeast proteome by multidimensional protein identification technology, *Nat. Biotechnol.*, 19 (2001) 242–247.
15 R.D. Macfarlane and D.F. Torgerson, Californium-252 plasma desorption mass spectrometry, *Science*, 191 (1976) 920.
16 M. Barber, R.S. Bordoli, R.D. Sedwick and A.N. Tyler, Fast atom bombardment of solids (FAB): A new ion source for mass spectrometry, *J. Chem. Soc. Chem. Commun.*, (1981) 325–327.
17 M. Dole, L.L. Mach, R.L. Hines, R.C. Mobley, L.D. Ferguson and M.B. Alice, Molecular beams of macroions, *J. Chem. Phys.*, 49 (1968) 2240–2249.
18 M. Yamashita and J.B. Fenn, Electrospray ion source: Another variation on the free-jet theme, *J. Phys. Chem.*, 88(20) (1984) 4451–4459.
19 M. Yamashita and J.B. Fenn, Negative ion production with the electrospray ion source, *J. Phys. Chem.*, 88 (1984) 4671–4675.
20 J.B. Fenn, M. Mann, C.K. Meng, S.F. Wong and C.M. Whitehouse, Electrospray ionization-principles and practice, *Mass Spectrom. Rev.*, 9(1) (1990) 37–70.
21 J.B. Fenn, Electrospray: Wings for molecular elephants, *(Nobel Lecture) Angew. Chem., Int. Ed.*, 42 (2003) 3871–3894.
22 M.L. Alexandrov, L.N. Gall, M.V. Krasnov, V.I. Nikolaev and V.A. Shkurov, *J. Anal. Chem. USSR*, 40 (1985) 1227–1236.

23 M. Mann, C.K. Meng and J.B. Fenn, Interpreting mass spectra of multiply charged ions, *Anal. Chem.*, 61(15) (1989) 1702–1708.
24 D.S. Ashton, C.R. Beddell, B.N. Green and R.W.A. Oliver, Rapid validation of molecular structures of biological samples by electrospray-mass spectrometry, *FEBS Lett.*, 342(1) (1994) 1–6.
25 P.H. Dawson, *Quadrupole Mass Spectrometry and its Applications*, Elsevier Science Publisher, New York, 1976.
26 W. Paul and H. Steinwedel, A new mass spectrometer without magnetic field, *Z. Naturforsch.*, 8a (1953) 448–450.
27 R.E. March and R.J. Hughes, *Quadrupole Storage Mass Spectrometry*, Wiley, New York, 1989.
28 J.F. Todd and R.E. March, *Practical Aspects of Ion Trap Mass Spectrometry-Volume I: Fundamentals of Ion Trap Mass Spectrometry*, CRC Press, Boca Raton, 1995, ISBN 0-8493-4452-2.
29 J.F. Todd and R.E. March, *Practical Aspects of Ion Trap Mass Spectrometry-Volume II: Ion Trap Instrumentation*, CRC Press, Boca Raton, 1995, ISBN 0-8493-8253-X.
30 J.F. Todd and R.E. March, *Practical Aspects of Ion Trap Mass Spectrometry-Volume III: Chemical, Environmental, and Biomedical Applications*, CRC Press, Boca Raton, 1995, ISBN 0-8493-8251-3.
31 J.F. Todd and R.E. March, *Quadrupole Ion Trap Mass Spectrometry*, 2nd ed., Wiley-Interscience, New York, 2005, ISBN 0-471-48888-7.
32 G.C. Stafford, P.E. Kelley, J.E.P. Syka, W.E. Reynolds and J.F.J. Todd, Recent improvements in and analytical applications of advanced ion trap technology, *Int. J. Mass Spectrom. Ion Process.*, 60(1) (1984) 85–98.
33 J.C. Schwartz, M.W. Senko and J.E.P. Syka, A Two-dimensional quadrupole ion trap mass spectrometer, *J. Am. Soc. Mass Spectrom.*, 13 (2002) 659–669.
34 R.T. McIver and J.R. McIver, *Fourier Transform Mass Spectrometry: Principles and Applications*. Ionspec Corporation, Irvine, California, USA, 2006.
35 J.D. Baldeschwieler, Ion cyclotron resonance spectroscopy. Cyclotron double resonance provides a new technique for the study of ion-molecule reaction mechanisms, *Science*, 159 (1968) 263.
36 M.B. Comisarow and A.G. Marshall, Fourier transform ion cyclotron resonance spectroscopy, *Chem. Phys. Lett.*, 25(2) (1974) 282–283.
37 R.T. McIver, R.L. Hunter and W.D. Bowers, Coupling a quadrupole mass spectrometer and a fourier transform mass spectrometer, *Int. J. Mass Spectrom. Ion Phys.*, 64 (1985) 67–77.
38 K.H. Kingdon, A method for the neutralization of electron space charge by positive ionization at very low gas pressures, *Phys. Rev.*, 21(4) (1923) 408–418.
39 R.D. Knight, Storage of ions from laser-produced plasmas, *Appl. Phys. Lett.*, 38 (1981) 221–223.
40 A. Makarov, Electrostatic axially harmonic orbital trapping: A high-performance technique of mass analysis, *Anal. Chem.*, 72 (2000) 1156.
41 Q. Hu, R.J. Noll, H. Li, A. Makarov, M. Hardman and G. Cooks, The orbitrap: A new mass spectrometer, *J. Mass Spectrom.*, 40(4) (2005) 430–443.
42 A. Makarov, Theory and practice of the orbitrap mass analyzer. *Proceedings of the 54th ASMS Conference on Mass Spectrometry and Allied Topics*, Seattle, Washington, USA, 2006.
43 J.V. Olsen, L.M.F. de Godoy, G. Li, B. Macek, P. Mortensen, R. Pesch, A. Makarov, O. Lange, S. Horning and M. Mann, Parts per million mass accuracy on an orbitrap mass spectrometer via lock mass injection into a C-trap, *Mol. Cell Proteomics*, 4(12) (2005) 2010–2021.
44 K.F. Faull, P.J. Anderson, J.D. Barchas and P.A. Berger, Selected ion monitoring assay for biogenic amine metabolites and probenecid in human cerebrospinal fluid, *J. Chromatogr. B, Biomed. Appl.*, 163 (1979) 337–349.
45 J.M. Wells and S.A. McLuckey, Collision-induced dissociation (CID) of peptides and proteins, *Methods Enzymol.*, 402 (2005) 148–185.
46 B. Paizs and S. Suhai, Fragmentation pathways of protonated peptides, *Mass Spectrom. Rev.*, 24(4) (2005) 508–548.
47 A.G. Harrison, A.B. Young, C. Bleiholder, S. Suhai and B. Paizs, Scrambling of sequence information in collision-induced dissociation of peptides, *J. Am. Chem. Soc.*, 128(32) (2006) 10364–10365.
48 L. Mouls, J.L. Aubagnac, J. Martinez and C. Enjalbal, Low energy peptide fragmentations in an ESI-Q-Tof type mass spectrometer, *J. Proteome Res.*, 6(4) (2007) 1378–1391.

49 L. Mouls, G. Subra, J.L. Aubagnac, J. Martinez and C. Enjalbal, Tandem mass spectrometry of amidated peptides, *J. Mass Spectrom.*, 41(11) (2006) 1470–1483.
50 X. Chen and F. Turecek, Simple b ions have cyclic oxazolone structures. A neutralization-reionization mass spectrometric and computational study of oxazolone radicals, *J. Am. Soc. Mass Spectrom.*, 16(12) (2005) 1941–1956.
51 R. Bakhtiar and Z. Guan, Electron capture dissociation mass spectrometry in characterization of peptides and proteins, *Biotechnol. Lett.*, 28(14) (2006) 1047–1059.
52 F.W. McLafferty, E.K. Fridriksson, D.M. Horn, M.A. Lewis and R.A. Zubarev, Biomolecule mass spectrometry, *Science*, 284(5418) (1999) 1289–1290.
53 L.M. Mikesh, B. Ueberheide, A. Chi, J.J. Coon, J.E. Syka, J. Shabanowitz and D.F. Hunt, The utility of ETD mass spectrometry in proteomic analysis, *Biochim. Biophys. Acta*, 1764(12) (2006) 1811–1822.
54 R.A. Zubarev, Electron-capture dissociation tandem mass spectrometry, *Curr. Opin. Biotechnol.*, 15(1) (2004) 12–16.
55 H.J. Cooper, Investigation of the presence of b ions in electron capture dissociation mass spectra, *J. Am. Soc. Mass Spectrom.*, 16(12) (2005) 1932–1940.
56 S. Lee, S.Y. Han, T.G. Lee, G. Chung, D. Lee and H.B. Oh, Observation of pronounced b∗,y cleavages in the electron capture dissociation mass spectrometry of polyamidoamine (PAMAM) dendrimer ions with amide functionalities, *J. Am. Soc. Mass Spectrom.*, 17(4) (2006) 536–543.
57 R.A. Zubarev, D.M. Horn, E.K. Fridricksson, N.L. Kelleher, N.A. Kruger, M.A. Lewis, B.K. Carpenter and F.W. McLafferty, Electron capture dissociation for structural characterization of multiply charged protein cations, *Anal. Chem.*, 72(3) (2000) 563–573.
58 N.L. Kelleher, R.A. Zubarev, K. Bush, B. Furie, B.C. Furie, F.W. McLafferty and C.T. Walsh, Localization of labile posttranslational modifications by electron capture dissociation: The case of gamma-carboxyglutamic, *Anal. Chem.*, 71(19) (1999) 4250–4253.
59 R. Bakhtiar and Z. Guan, Electron capture dissociation mass spectrometry in characterization of post-translational modifications, *Biochem. Biophys. Res. Commun.*, 334(1) (2005) 1–8.
60 K. Breuker and F.W. McLafferty, Native electron capture dissociation for the structural characterization of noncovalent interactions in native cytochrome C, *Angew. Chem. Int. Ed. Engl.*, 42(40) (2003) 4900–4904.
61 Y.O. Tsybin, M. Ramstrom, M. Witt, G. Baykut and P. Hakansson, Peptide and protein characterization by high-rate electron capture dissociation Fourier transform ion cyclotron resonance mass spectrometry, *J. Mass Spectrom.*, 39(9) (2004) 1077.
62 Y. Xie, J. Zhang, S. Yin and J.A. Loo, Top-down ESI-ECD-FT-ICR mass spectrometry localizes noncovalent protein-ligand binding sites, *J. Am. Chem. Soc.*, 128(45) (2006) 14432–14433.
63 J.J. Coon, B. Ueberheide, J.E. Syka, D.D. Dryhurst, J. Ausio, J. Shabanowitz and D.F. Hunt, Protein identification using sequential ion/ion reactions and tandem mass spectrometry, *Proc. Natl. Acad. Sci. USA*, 102(27) (2005) 9463–9468.
64 J.E. Syka, J.J. Coon, M.J. Schroeder, Shabanowitz and D.F. Hunt, Peptide and protein sequence analysis by electron transfer dissociation mass spectrometry, *Proc. Natl. Acad. Sci. USA*, 101(26) (2004) 9528–9533.
65 R.J. Chakley, C.S. Brinkworth and A.L. Burlingame, Side-chain fragmentation of alkylated cysteine residues in electron capture dissociation mass spectrometry, *J. Am. Soc. Mass Spectrom.*, 17(9) (2006) 1271–1274.